Optimal control strategies for the reliable and competitive mathematical analysis of Covid-19 pandemic model

A.I.K. Butt*, M. Imran†, D.B.D. Chamaleen‡, S. Batool§

Abstract

To understand dynamics of the COVID-19 disease realistically, a new SEIAPHR model has been proposed in this article where the infectious individuals have been categorized as symptomatic, asymptomatic and super-spreaders. The model has been investigated for existence of a unique solution. To measure the contagiousness of COVID-19, reproduction number $\mathcal{R}_0$ is also computed using next generation matrix method. It is shown that model is locally stable at disease free equilibrium point when $\mathcal{R}_0 < 1$ and unstable for $\mathcal{R}_0 > 1$. The model has been analyzed for global stability at both of the disease free and endemic equilibrium points. Sensitivity analysis is also included to examine the effect of parameters of the model on reproduction number $\mathcal{R}_0$. Couple of optimal control problems have been designed to study the effect of control strategies for disease control and eradication from the society. Numerical results show that the adopted control approaches are much effective in reducing new infections.

Keywords: COVID-19; Local and global stabilities; Existence and uniqueness; Sensitivity analysis; Non-pharmaceutical; Pontryagin maximum principle; Optimal control.

1 Introduction

In December 2019, a new kind of Corona virus was experienced in Wuhan (China). This new type of virus embraced the whole city in few days and later on spread over the whole world in a very short span of time. The new virus was named as Covid-19 by World Health Organization (WHO) and disease due to virus was declared as pandemic in March, 2020 [1]-[2]. According to WHO, Covid-19 transmitted from snake and bats to human population through seafood market of Wuhan. The deathly virus not only troubled the entire world in the fields related to health but also ruined the world economy, education system and social life of humans. As of 28 December 2021, WHO reported that the Corona virus has infected more than 280,119,931 confirmed cases with 5,403,662 deaths. With the new variants like Delta and Omicron, the number of confirmed cases are continuously increasing. Omicron has the capability to spread quickly as compared to other variants. Lot of investigations are being carried out to determine the transmissibility and severity of Omicron. However, more than 220, 951, 891 individuals have also been recovered from deadly disease and its variants.

Dry cough, sneezing, trouble in breathing, headache, fatigue,loss of smell and taste, vomiting, sore throat and body pain are usual symptoms of Covid-19. Covid-19 damages the human's lungs, liver and kidney etc. The mortality caused by Covid-19 rates differently in different countries depending on the environment and food situation of the countries [1]-[3], [7]-[16]. The mortality rate also relies upon the ratio of young and old people. The people over the age of 60 and having diseases like diabetes, cancer, cardiac, obesity, blood pressure, lungs issues are at high risk of

*Department of Mathematics, GC University, Lahore, Pakistan. Email: azhar.butt@gcu.edu.pk
†Department of Mathematics, GC University, Lahore, Pakistan. Email: m.imran4170@gmail.com
‡Department of Mathematics, GC University, Lahore, Pakistan. Email: chamaleen1991@gmail.com
§Department of Mathematics, GC University, Lahore, Pakistan. Email: batoolsaira991@gmail.com

getting a severe infection that may end up with death [17]-[21]. Covid-19 has an incubation period of 2 to 14 days [22].

Dynamics of the disease and its transmission patterns are continuously being observed by both the public health experts and policy makers to suggest appropriate solutions for disease control and eradication. The foremost step in case of Covid-19 is to run awareness and self-protection campaigns in the community. For instance, the general public should be educated to wear face masks, to avoid large indoor gatherings, to keep social distance of at leat 6 feet, to wash hands for at least 20 seconds. Other precautionary measures include smart lock down strategy, isolating exposed or infected individuals, vaccinating the susceptible individuals.

In the field of mathematical modeling and optimal control design, researchers are continuously trying to develop different mathematical models of Covid-19 according to physical situations or requirements and are presenting a variety of control strategies for disease control [7]-[26]. In this study, we design a new Covid-19 model termed as SEIAPHR where the infectious humans are placed in three compartments such as symptomatic infected I, asymptomatic A, and super-spreaders P. The division of infectious individuals in three compartments makes the model more realistic for the sake of analysis and control of disease. To restrict the spread of Covid-19 in human population, a few of non-pharmaceutical strategies such as quarantine, health awareness, self protection, social distancing are also proposed and incorporated in the Covid-19 SEIAPHR model.

Rest of the article is managed as follows: Section 2 deals with the formulation of a nonlinear coupled mathematical model for Covid-19. Fixed point theorem is implemented to prove existence of a unique solution in section 3. The model is made more reliable and realistic by showing positivity and boundedness of the state variables in section 4. The disease free equilibrium (DFE) point and the endemic equilibrium (EE) point are also calculated in section 5. In section 6, next generation approach is employed to determine the reproduction number $\mathcal{R}_0$. Both the local and global stabilities at equilibrium points are examined in section 7. Section 8 is devoted for the sensitivity analysis of the parameters involved in reproduction number.

As a first optimal control strategy, the model SEIAPHR is reformulated in section 9 to adjust a class of quarantined people Q(t). With the isolation strategy for disease control, the optimal control problem is designed and solved numerically in section 9. The corresponding graphical results are also illustrated here. As a second non-pharmaceutical control strategy, the SEIAPHR model is once again updated in section 10 to include three additional parameters (controls) named as public health information, personal protection and medication. The corresponding optimal control problem is also formulated in this section. Optimality conditions are also derived and solved numerically for presentation of graphical results. The findings of the study are summarized in section 11.

2 Design for Covid-19 model

In the field of epidemiology, mathematical models play pivotal role in understanding the disease transmission dynamics. A carefully designed model helps the policy makers to foresee the disease patterns and to make right decisions in restricting the spread of disease. In this section, we design a new realistic SEIAPHR model where we have categorized the infectious individuals into three classes named symptomatic, asymptomatic and super-spreaders. In the first place our focus is to study the disease dynamics by analyzing the model mathematically and then to suggest some control strategies to optimally control the disease.

We categorize the total population $N(t)$ into seven classes as follows: susceptible $S(t)$, exposed $E(t)$, symptomatically infected $I(t)$, asymptomatic $A(t)$, super-spreader $P(t)$, hospitalized $H(t)$ and recovered $R(t)$. Therefore, the whole population $N(t)$ at any time t is given as

$$N(t) = S(t) + E(t) + I(t) + A(t) + P(t) + H(t) + R(t). \tag{1}$$

The first class is known as the susceptible class, denoted by $S(t)$. In this class, we consider those individuals who are at risk and can easily be infected after the transmittable interaction with infectious individuals. When a person of susceptible class has such an interaction, the person will move in exposed class. The exposed class, denoted by $E(t)$, is restrained for those who are infected but not infectious yet. In this class pathogenic microbiological agent develops and consistently strengthen. Then, third class comes up from the exposed class containing those who are now infectious and experiencing the symptoms of corona disease identified as an symptomatic infected class, denoted by $I(t)$. The fourth compartment comprises those particular group of exposed individuals who are infectious now but they are not facing the signs of corona disease, known as asymptomatic class. This class is denoted by $A(t)$. The fifth one is named as super-spreader class in which we have considered those who are the rapid carrier of virus e.g. public transporter, salespersons, delivery staff and shopkeepers etc. This category is represented by $P(t)$. The patients with severe health conditions are forming the hospitalized class. This class is indicated by $H(t)$. In the end, people who recovered with medicated treatment or by their strong immune system will lie in the recovered class symbolized by $R(t)$. It is also assumed that the recovered individuals will occupy this class for the whole life. The real valued state variables S, E, I, A, P, H, R are also considered to be continuously differentiable functions of $t \in [0, \infty)$. Figure 1 explains the flow pattern of disease in the above said compartments.

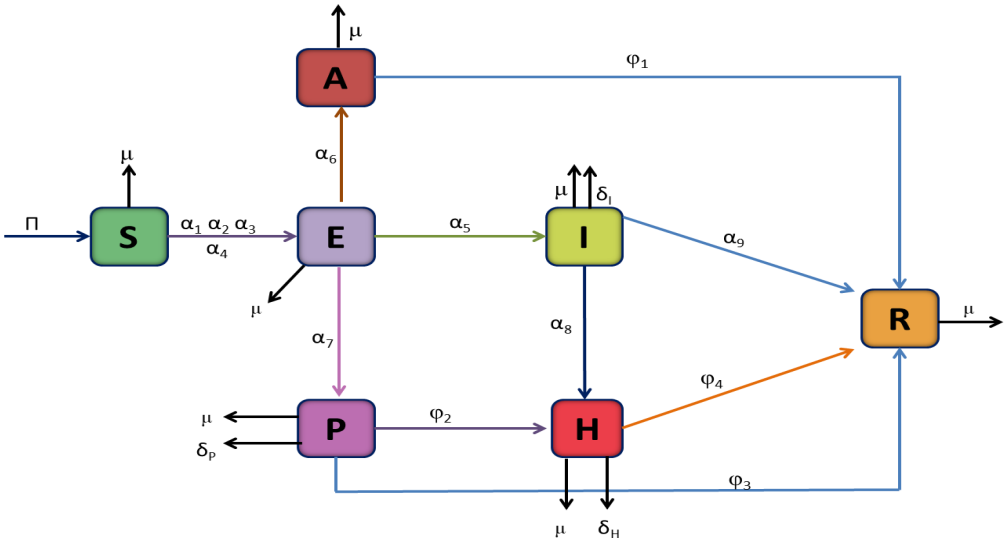

Figure 1: Flow diagram of Covid-19 disease transmission.

Mathematically, disease flow pattern is described in the form of following non-linear coupled

ordinary differential equations, called SEIAPHR model.

$$\frac{dS}{dt} = \Pi - \frac{(\alpha_1 I + \alpha_2 A + \alpha_3 P + \alpha_4 H)S}{N} - \mu S, \tag{2a}$$

$$\frac{dE}{dt} = \frac{(\alpha_1 I + \alpha_2 A + \alpha_3 P + \alpha_4 H)S}{N} - (\alpha_5 + \alpha_6 + \alpha_7 + \mu)E, \tag{2b}$$

$$\frac{dI}{dt} = \alpha_5 E - (\alpha_8 + \alpha_9 + \mu + \delta_I)I, \tag{2c}$$

$$\frac{dA}{dt} = \alpha_6 E - (\varphi_1 + \mu)A, \tag{2d}$$

$$\frac{dP}{dt} = \alpha_7 E - (\varphi_2 + \varphi_3 + \mu + \delta_P)P, \tag{2e}$$

$$\frac{dH}{dt} = \alpha_8 I + \varphi_2 P - (\varphi_4 + \delta_H + \mu)H, \tag{2f}$$

$$\frac{dR}{dt} = \alpha_9 I + \varphi_1 A + \varphi_3 P + \varphi_4 H - \mu R, \tag{2g}$$

with non-negative initial conditions:

$$\begin{aligned} &S(0) = S_0, \quad E(0) = E_0, \quad I(0) = I_0, \quad A(0) = A_0, \\ &P(0) = P_0, \quad H(0) = H_0, \quad R(0) = R_0. \end{aligned} \tag{2h}$$

The values and physical interpretation of the parameters considered in the model (2) are given in the Table 1.

Parameter	Description	Values	Source
α_1	Transmission rate from S to E due to contact with I	0.866	Assumed
α_2	Transmission rate from S to E due to contact with A	0.16	[10]
α_3	Transmission rate from S to E due to contact with P	0.8	Assumed
α_4	Transmission rate from S to E due to contact with H	0.0131	[10]
α_5	Transmission rate from E to I	0.235	[10]
α_6	Transmission rate from E to A	0.26	[10]
α_7	Transmission rate from E to P	0.56	Assumed
α_8	Transmission rate from I to H	0.45	[10]
α_9	Transmission rate from I to R	0.6381	[10]
φ_1	Transmission rate from A to R	0.08	[10]
φ_2	Transmission rate from P to R	0.1	Assumed
φ_3	Transmission rate from P to R	0.3	Assumed
φ_4	Transmission rate from H to R	0.5431	[10]
δ_I	Death rate due to disease in I	0.08	Assumed
δ_Q	Death rate due to disease in Q	0.01	[10]
δ_P	Death rate due to disease in P	0.0412	Assumed
δ_H	Death rate due to disease in H	0.485	Assumed
Π	Birth rate	2.5	Assumed
μ	Natural death rate	0.241	Assumed

Table 1: Parametric values.

3 Existence and uniqueness of solution

In this section, we state some theorems to prove existence and uniqueness of solution of the Covid-19 model (2). Some basic definitions and theorems from functional analysis are also presented here to support the proof of our stated theorems.

Let us put the Covid-19 model (2) in the form

$$\frac{dy}{dt} = g(t, y), \tag{3a}$$

$$y(0) = y_0, \tag{3b}$$

where $y : R_+ \to R_+^7$ is a real valued function defined by

$$y(t) = (S(t), E(t), I(t), A(t), P(t), H(t), R(t))^T,$$

with

$$y_0 = (S(0), E(0), I(0), A(0), P(0), H(0), R(0))^T,$$

and

$$g(t, y) = (g_1(t, y), g_2(t, y), g_3(t, y), g_4(t, y), g_5(t, y), g_6(t, y), g_7(t, y))^T,$$

where $g_i(t, y),\ i = 1, 2, \ldots, 7$ are right hand sides of the equations of model (2). To establish existence and uniqueness of the solution of model (2), we state some basic theorems and definitions.

Theorem 1 *[27] Let $h : D \to R^n$ be a continuously differentiable mapping from $D \subseteq R$ to R^n. Then h satisfies a Lipschitz condition on each convex compact subset $\mathcal{D}$ of D with Lipchitz constant K. Where K is the supremum of the derivative of h on $\mathcal{D}$, i.e.,*

$$K = \sup_{x \in \mathcal{D}} \mid \frac{dh}{dx} \mid$$

□

Theorem 2 *[28] Suppose $D = \{(t, z) | t \in R, z \in R^n\}$, and let $h(t, z)$ be continuous on D and satisfies Lipschitz condition there, then the initial value problem*

$$\frac{dz}{dt} = h(t, z),\ z(t_0) = z_0.$$

has a solution. □

Definition 1 *Picard Mapping [27] Given a point $(t_0, z_0) \in R \times R^n$ and a differential equation*

$$\frac{dz}{dt} = h(t, z),$$

where $z \in R^n$ and h is a vector field over $R \times R^n$, identify Picard mapping towards mapping ψ that takes a function $\phi : t \to z$ to the function $\psi\phi : t \to z$, such as

$$(\psi\phi)(t) = z_0 + \int_{t_0}^{t} h(\tau, \phi(\tau))d\tau,$$

with

$$(\psi\phi)(t_0) = z_0.$$

□

Theorem 3 *[27] The mapping $\phi : R \to R^n$ is a solution to*

$$\frac{dz}{dt} = h(t, z),$$

with initial condition

$$\phi(t_0) = z_0,$$

if and only if

$$\psi\phi = \phi.$$

Where

$$(\psi\phi)(t) = z_0 + \int_{t_0}^{t} h(\tau, \phi(\tau))d\tau,$$

with

$$(\psi\phi)(t_0) = z_0.$$

□

Theorem 4 *The right hand side function g in* (3a) *is Lipschitz continuous in y.*

Proof: Let V be a convex compact subset of

$$D = \{(t, y)|\ t_0 \leq t \leq t_f,\ y \in R_+^7\}.$$

Let $(t, \bar{y}_1), (t, \bar{y}_2) \in V$, then by mean value theorem (for several variables) $\exists\ \zeta \in (\bar{y}_1, \bar{y}_2)$ such that

$$\frac{g(t, \bar{y}_1) - g(t, \bar{y}_2)}{\bar{y}_1 - \bar{y}_2} = g'(t, \zeta),$$

where

$$g'(t, \zeta) = \sum_{i=1}^{7} \frac{\partial g(t, \zeta)}{\partial y_i}.$$

Hence

$$g(t, \bar{y}_1) - g(t, \bar{y}_2) = \sum_{i=1}^{7} \frac{\partial g(t, \zeta)}{\partial y_i}.(\bar{y}_1 - \bar{y}_2).$$

$$\begin{aligned} |\ g(t, \bar{y}_1) - g(t, \bar{y}_2)\ | &= |\ \sum_{i=1}^{7} \frac{\partial g(t, \zeta)}{\partial y_i}.(\bar{y}_1 - \bar{y}_2)\ |, \\ &\leq \|\sum_{i=1}^{7} \frac{\partial g(t, \zeta)}{\partial y_i}\| \|(\bar{y}_1 - \bar{y}_2)\|. \end{aligned}$$

Since $g \in C^1$, hence over convex compact set V, $\exists$ constant $\alpha > 0$ such that

$$\|\sum_{i=1}^{7} \frac{\partial g(t, \zeta)}{\partial y_i}\| \leq \alpha,$$

hence

$$\begin{aligned} |\ g(t, \bar{y}_1) - g(t, \bar{y}_2)\ | &\leq \alpha \|(\bar{y}_1 - \bar{y}_2)\| \\ \sup_{t \in [0, t_f]} |\ g(t, \bar{y}_1) - g(t, \bar{y}_2)\ | &\leq \alpha \sup_{t \in [0, t_f]} \|(\bar{y}_1 - \bar{y}_2)\| \\ \|g(t, \bar{y}_1) - g(t, \bar{y}_2)\|_\infty &\leq \alpha \|\bar{y}_1 - \bar{y}_2\|_\infty \end{aligned}$$

Hence, $g(t, y)$ is Lipschitz in second argument. □

Thus theorem 2 implies that system (3) has a solution and theorem 3 implies that solution will be the fixed point of Picard mapping.

Theorem 5 *[29] Let M be a complete metric space and $\psi : X \to X$ be a contraction on X. Then ψ has one and only one fixed point.* □

Theorem 6 *The solution of model* (3) *is unique.*

Proof: To prove the uniqueness of solution, we suppose that ϕ_1 and ϕ_2 be two solutions of (3). Then, both will be the fixed points of the Picard mapping, i.e.,

$$\begin{aligned}\psi\phi_1(t) &= \phi_1(t),\\ &= z_0 + \int_0^t g(\tau, \phi_1(\tau))d\tau,\end{aligned}$$

and

$$\begin{aligned}\psi\phi_2(t) &= \phi_2(t),\\ &= z_0 + \int_0^t g(\tau, \phi_2(\tau))d\tau.\end{aligned}$$

Thus,

$$\begin{aligned}| \psi\phi_1(t) - \psi\phi_2(t) | &= | \int_0^t g(\tau, \phi_1(\tau))d\tau - \int_0^t g(\tau, \phi_2(\tau))d\tau |,\\ &\leq \int_0^t |g(\tau, \phi_1(\tau))dt - g(\tau, \phi_2(\tau))|dt.\\ \sup_{t\in[0,t_f]} | \psi\phi_1(t) - \psi\phi_2(t) | &\leq \int_0^t \sup_{\tau\in[0,t_f]} |g(\tau, \phi_1(\tau))dt - g(\tau, \phi_2(\tau))|dt.\end{aligned}$$

As g satisfies the Lipschitz condition in the second argument, so

$$\begin{aligned}\|\psi\phi_1 - \psi\phi_2\|_\infty &\leq \int_0^t \alpha\|\phi_1 - \phi_2\|_\infty d\tau,\\ &\leq \int_0^{t_f} \alpha\|\phi_1 - \phi_2\|_\infty d\tau,\\ &\leq \alpha\|\phi_1 - \phi_2\|_\infty \int_0^{t_f} dt,\\ &\leq \alpha\|\phi_1 - \phi_2\|_\infty t_f,\\ &\leq t_f\alpha\|\phi_1 - \phi_2\|_\infty.\end{aligned}$$

If we choose $t_f < \dfrac{1}{\alpha}$, the mapping is contraction. Here, t_f represents the final time and α is the Lipchitz constant.

Hence, Theorem 5 implies uniqueness of the solution of SEIAPHR model (2). □

4 Boundedness and positivity of solutions

In this section, we prove boundedness and positivity of the state variables of model (2) and also define the feasible region for the state variables.

Theorem 7 *The solution y(t) of Covid-19 model* (2) *is bounded.*

Proof: Differentiating equation (1) with respect to time t and then using equations of model (2), we obtain

$$\frac{dN}{dt} = \Pi - (\delta_I I + \delta_P P + \delta_H H) - \mu N, \tag{4}$$

with

$$N(0) = S(0) + E(0) + I(0) + A(0) + P(0) + H(0) + R(0).$$

Suppose for any initial condition, we have

$$N(0) \leq \frac{\Pi}{\mu}. \tag{5}$$

Equation (4) can be put in the form:

$$\frac{dN}{dt} \leq \Pi - \mu N. \tag{6}$$

By using Grönwall's inequality, (6) is solved to reach at the solution

$$N(t) \leq \frac{\Pi}{\mu} + \left(N(0) - \frac{\Pi}{\mu}\right) exp\,(-\mu t),$$

which implies that

$$N(t) \leq \frac{\Pi}{\mu}, \text{ for all } t \geq 0.$$

Hence, it is proved that

$$\lim_{t\to\infty} N(t) \leq \frac{\Pi}{\mu}.$$

Thus, the solution $y(t)$ is bounded for every $t \geq 0$. □

Theorem 8 *The solution $y(t)$ of system of equations* (2) *having non-negative initial conditions* (2h) *is positive for all $t \geq 0$.*

Proof: First suppose that

$$y(0) \geq 0.$$

The equation (2.1.2a) could be written in the form

$$\frac{dS}{dt} + \left(\frac{\alpha_1 I + \alpha_2 A + \alpha_3 P + \alpha_4 H}{N} + \mu\right) S = \Pi, \tag{7}$$

Since the solutions of the model (2) are bounded, so equation (7) can be put in the form

$$\frac{dS}{dt} + (\rho(t) + \mu)\, S = \Pi, \tag{8}$$

where

$$\rho(t) = \frac{\alpha_1 I + \alpha_2 A + \alpha_3 P + \alpha_4 H}{N}.$$

Equation (8) is a linear in S whose integrating factor is computed to have $exp\left(\mu t + \int_0^t \rho(y)dy\right)$. So, equation (8) after multiplication with the integrating factor becomes.

$$\frac{d}{dt}\left[exp\left(\mu t + \int_0^t \rho(y)dy\right)S\right] = \Pi\ exp\left(\mu t + \int_0^t \rho(y)dy\right).$$

Integrating over the interval $[0, \bar{t}]$, where $\bar{t} = \max\{t > 0, z(t) > 0\}$, we get

$$S(\bar{t})\ exp\left(\mu\bar{t} + \int_0^{\bar{t}} \rho(y)dy\right) - S(0) = \Pi \int_0^{\bar{t}} exp\left(\mu t + \int_0^t \rho(y)dy\right)dt.$$

Simplification yields us

$$S(\bar{t}) = S(0)\ exp\left(-(\mu\bar{t} + \int_0^{\bar{t}} \rho(y)dy)\right) + exp\left(-(\mu\bar{t} + \int_0^{\bar{t}} \rho(y)dy)\right)\left(\Pi \int_0^{\bar{t}} exp\left(\mu t + \int_0^t \rho(y)dy\right)dt\right). \quad (9)$$

Since $S(0) \geq 0$, so (9) implies that $S(\bar{t}) > 0$ for all $\bar{t} \in [0, t]$. In the same way, we can prove that all the other state variables are positive. □

Thus the feasible region for the model is defined as follows:

$$\Omega = \Big\{(S, E, I, A, P, H, R) \in R_+^7 : 0 \leq N \leq \frac{\Pi}{\mu}\Big\}. \quad (10)$$

5 Equilibrium points

Equilibrium points are computed by solving steady-state equations of the model (2). For Corona free or DFE point, we consider the absence of virus whereas for Corona present or EE point, presence of virus is assumed in community.

Therefor, Corona free or the disease free equilibrium (DFE) point is computed to give:

$$\mathcal{P}_0 = \left(\frac{\Pi}{\mu}, 0, 0, 0, 0, 0, 0, 0\right), \quad (11)$$

and Corona present or the endemic equilibrium (EE) point is given as:

$$\mathcal{P}_1 = (S^1, E^1, I^1, A^1, P^1, H^1, R^1), \quad (12)$$

where

$$\begin{aligned}
S^1 &= \Big[\frac{N(\alpha_5 + \alpha_6 + \alpha_7 + \mu)}{\beta}\Big],\\
E^1 &= \Big[\frac{\Pi}{\alpha_5 + \alpha_6 + \alpha_7 + \mu} - \frac{\mu N}{\beta}\Big],\\
I^1 &= \frac{\alpha_5}{k_2}\Big[\frac{\Pi}{\alpha_5 + \alpha_6 + \alpha_7 + \mu} - \frac{\mu N}{\beta}\Big],\\
A^1 &= \frac{\alpha_6}{k_3}\Big[\frac{\Pi}{\alpha_5 + \alpha_6 + \alpha_7 + \mu} - \frac{\mu N}{\beta}\Big],\\
P^1 &= \frac{\alpha_7}{k_4}\Big[\frac{\Pi}{\alpha_5 + \alpha_6 + \alpha_7 + \mu} - \frac{\mu N}{\beta}\Big],\\
H^1 &= \frac{1}{k_5}\Big[\frac{\alpha_8\alpha_5}{k_2} + \frac{\varphi_2\alpha_7}{k_4}\Big][\frac{\Pi}{\alpha_5 + \alpha_6 + \alpha_7 + \mu} - \frac{\mu N}{\beta}\Big],\\
R^1 &= \frac{1}{\mu}\Big[\alpha_9 I^1 + \varphi_1 A^1 + \varphi_3 P^1 + \varphi_4 H^1\Big],
\end{aligned}$$

with

$$\begin{aligned}
\beta &= \frac{\alpha_1\alpha_5}{k_2} + \frac{\alpha_2\alpha_6}{k_3} + \frac{\alpha_3\alpha_7}{k_4} + \frac{\alpha_4}{k_5}(\frac{\alpha_8\alpha_5}{k_2} + \frac{\varphi_3\alpha_7}{k4}),\\
k_1 &= \alpha_5 + \alpha_6 + \alpha_7 + \mu,\\
k_2 &= \alpha_8 + \alpha_9 + \mu + \delta_I,\\
k_3 &= \varphi_1 + \mu,\\
k_4 &= \varphi_2 + \varphi_3 + \mu + \delta_P,\\
k_5 &= \varphi_4 + \mu + \delta_H.
\end{aligned}$$

6 Reproduction number

The reproduction number $\mathcal{R}_0$ is a mathematical quantity which determines the disease's dispersion. Disease is pandemic only in the case if $\mathcal{R}_0 > 1$. The number is computed using the next generation matrix method [9, 30, 31]. It is actually a spectral radius of FV^{-1}, where F is the jacobian of the rate of recruitment of new infections and V is the jacobian of the rate of the other transmission terms in equations involving infections. That is

$$F = \left(\frac{\partial \mathcal{F}_j}{\partial x_i}\right)_{\mathcal{P}_0}, \quad i, j = 1, 2, 3, 4, 5,$$

$$V = \left(\frac{\partial \mathcal{V}_j}{\partial x_i}\right)_{\mathcal{P}_0}, \quad i, j = 1, 2, 3, 4, 5.$$

where $x_i,\ i = 1, \ldots, 5$ respectively represent state variables E, I, A, P, H and

$$\mathcal{F} = \begin{pmatrix} \frac{(\alpha_1 I + \alpha_2 A + \alpha_3 P + \alpha_4 H)S}{N} \\ 0 \\ 0 \\ 0 \\ 0 \end{pmatrix},$$

$$\mathcal{V} = \begin{pmatrix} (\alpha_5 + \alpha_6 + \alpha_7 + \mu)E \\ -\alpha_5 E + (\alpha_8 + \alpha_9 + \mu + \delta_I)I \\ -\alpha_6 E + (\varphi_1 + \mu)A \\ -\alpha_7 E + (\varphi_2 + \varphi_3 + \mu + \delta_P)P \\ -\alpha_8 I - \varphi_2 P + (\varphi_4 + \delta_H + \mu)H \end{pmatrix}.$$

The absolute maximum eigenvalue of the matrix FV^{-1} is computed to give the reproduction number

$$\mathcal{R}_0 = \frac{\alpha_1\alpha_5 k_3 k_4 k_5 + \alpha_2\alpha_6 k_2 k_4 k_5 + \alpha_3\alpha_7 k_2 k_3 k_5 + \alpha_4\alpha_5\alpha_8 k_3 k_4 + \alpha_4\alpha_7 k_2 k_3 \varphi_2}{k_1 k_2 k_3 k_4 k_5}. \tag{13}$$

7 Stability analysis

This section deals with the local and global stabilities of the Covid-19 model (2) at the DEF and EE points. Global stabilities are investigated using the Lyapunov theory with LaSalle invariant principle [31] and Castillo-Chavez approach [32].

7.1 Local stability at DFE

Jacobian matrix method is computed for model (2) to evaluate its local stability at DFE. The jacobian matrix evaluated at $\mathcal{P}_0$ is given as

$$J_{\mathcal{P}_0} = \begin{pmatrix} -\mu & 0 & -\alpha_1 & -\alpha_2 & -\alpha_3 & -\alpha_4 & 0 \\ 0 & -k_1 & \alpha_1 & \alpha_2 & \alpha_3 & \alpha_4 & 0 \\ 0 & \alpha_5 & -k_2 & 0 & 0 & 0 & 0 \\ 0 & \alpha_6 & 0 & -k_3 & 0 & 0 & 0 \\ 0 & \alpha_7 & 0 & 0 & -k_4 & 0 & 0 \\ 0 & 0 & \alpha_8 & 0 & \varphi_2 & -k_5 & 0 \\ 0 & 0 & \alpha_9 & \varphi_1 & \varphi_3 & \varphi_4 & -\mu \end{pmatrix}. \tag{14}$$

We present the following theorem for local stability of the model (2) at DFE point $\mathcal{P}_0$.

Theorem 9 *The model* (2) *is locally asymptotically stabile (LAS) at* $\mathcal{P}_0$ *if* $\mathcal{R}_0 < 1$ *and unstable for* $\mathcal{R}_0 > 1$.

Proof: With the assistance of Maple software, we attain the following eigenvalues of the jacobian matrix (14).

$$\lambda_1 = -\mu, \tag{15a}$$
$$\lambda_2 = -\mu, \tag{15b}$$
$$\lambda_3 = -k_1, \tag{15c}$$
$$\lambda_4 = -\frac{k_1k_2 - \alpha_1\alpha_5}{k_1}, \tag{15d}$$
$$\lambda_5 = -\frac{(k_1k_2k_3k_4k_5)(1-\mathcal{R}_0) + N_1}{k_4k_5(\lambda_3\lambda_4)}, \tag{15e}$$
$$\lambda_6 = -\frac{(1-\mathcal{R}_0)k_1k_2k_3k_4k_5 + N_2}{k_1k_5(\lambda_3\lambda_4}, \tag{15f}$$
$$\lambda_7 = -\frac{(1-\mathcal{R}_0)}{\lambda_3\lambda_4\lambda_5\lambda_6}, \tag{15g}$$

where,

$$N_1 = k_2k_3k_5\alpha_3\alpha_7 + k_3k_4\alpha_4\alpha_5\alpha_8 + k_2k_3\alpha_4\alpha_7\varphi_2,$$
$$N_2 = k_3k_4\alpha_4\alpha_5\alpha_8 + k_2k_3\alpha_4\alpha_7\varphi_2.$$

It is evident from (15) that all the eigenvalues are negative when $\mathcal{R}_0 < 1$ but not in the case when $\mathcal{R}_0 > 1$. Thus, it is proved that model (2) is LAS for $\mathcal{R}_0 < 1$ and unstable for $\mathcal{R}_0 > 1$. □

7.2 Global stability

In order to show that DFE point $\mathcal{P}_0$ is globally stable, we use the approach given by Castillo-Chavez et al. and re-write the model (2) in the form

$$\begin{aligned} \frac{d\mathcal{Y}}{dt} &= \mathcal{K}(\mathcal{X},\mathcal{Y}), \\ \frac{d\mathcal{Y}}{dt} &= \mathcal{N}(\mathcal{X},\mathcal{Y}), \quad \mathcal{N}(\mathcal{X},0) = 0, \end{aligned} \tag{16}$$

where $\mathcal{X} = (S)$ represents uninfected humans who are susceptible and $\mathcal{Y} = (E, I, A, P, H)$ denotes the number of people who are exposed, symptomatic, asymptomatic, super-spreader, and hospitalized, with $\mathcal{X} \in \mathbb{R}_+$ and $\mathcal{Y} \in \mathbb{R}^5_+$. We omit the model's last equation since it is independent to the others. $\mathcal{P}_0 = (\mathcal{X}_0, 0) = \left(\frac{\Pi}{\mu}, 0, 0, 0, 0, 0\right)$ is the DFE point. To prove the global asymptotical stability (GAS) of disease-free equilibrium point, the conditions given below must be fulfilled.

$$(H1) \quad \frac{d\mathcal{X}}{dt} = \mathcal{K}(\mathcal{X}, 0) = 0, \ \mathcal{X}_0 \text{ is } GAS, \tag{17}$$
$$(H2) \quad \frac{d\mathcal{Y}}{dt} = \mathcal{N}(\mathcal{X},\mathcal{Y}) = \mathcal{B}\mathcal{Y} - \bar{\mathcal{N}}(\mathcal{X},\mathcal{Y}) \text{ where } \bar{\mathcal{N}}(\mathcal{X},\mathcal{Y}) \geq 0 \text{ for all } (\mathcal{X},\mathcal{Y}) \in \Omega. \tag{18}$$

Here, $\mathcal{B} = D_{\mathcal{Y}}\mathcal{N}(\mathcal{X}_0, 0)$ is an M-matrix and Ω is the model's feasible region. Thus, due to Castillo-Chavez et al., we state the following theorem.

Theorem 10 *The DFE point* $\mathcal{P}_0$ *of the model* (2) *is GAS if* $\mathcal{R}_0 < 1$ *and the conditions* $(H1)$ *and* $(H2)$ *are met.*

Proof: Let $\mathcal{X} = (S)$ represents uninfected persons, $\mathcal{Y} = (E, I, A, P, H)$ represent exposed, symptomatic infected, asymptomatic, super-spreader and hospitalized individuals and $\mathcal{P}_0 = (\mathcal{X}_0, 0)$ is the disease-free equilibrium point. So

$$\frac{d\mathcal{X}}{dt} = \mathcal{K}(\mathcal{X}, \mathcal{Y}) = \Pi - (\alpha_1 I + \alpha_2 A + \alpha_3 P + \alpha_4 H)\frac{S}{N} - \mu S. \tag{19}$$

If $S = S_0$, then $\mathcal{K}(\mathcal{X}, 0) = 0$, i.e.,

$$\frac{d\mathcal{X}}{dt} = \Pi - \mu S_0 = 0. \tag{20}$$

From equation (20) as $t \to \infty$, $\mathcal{X} \to \mathcal{X}_0$. Therefore $\mathcal{X}_0 = (S_0, 0)$ is GAS. Now,

$$\mathcal{B}\mathcal{Y} - \bar{\mathcal{N}}(\mathcal{X}, \mathcal{Y}) = \begin{bmatrix} -k_1 & \frac{\alpha_1 S_0}{N} & \frac{\alpha_2 S_0}{N} & \frac{\alpha_3 S_0}{N} & \frac{\alpha_4 S_0}{N} \\ \alpha_5 & -k_2 & 0 & 0 & 0 \\ \alpha_6 & 0 & -k_3 & 0 & 0 \\ \alpha_7 & 0 & 0 & -k_4 & 0 \\ 0 & \alpha_8 & 0 & \varphi_2 & -k_5 \end{bmatrix} \begin{bmatrix} E \\ I \\ A \\ P \\ H \end{bmatrix} - \begin{bmatrix} \kappa \\ 0 \\ 0 \\ 0 \\ 0 \end{bmatrix}. \tag{21}$$

where

$$\mathcal{B} = \begin{bmatrix} -k_1 & \frac{\alpha_1 S_0}{N} & \frac{\alpha_2 S_0}{N} & \frac{\alpha_3 S_0}{N} & \frac{\alpha_4 S_0}{N} \\ \alpha_5 & -k_2 & 0 & 0 & 0 \\ \alpha_6 & 0 & -k_3 & 0 & 0 \\ \alpha_7 & 0 & 0 & -k_4 & 0 \\ 0 & \alpha_8 & 0 & \varphi_2 & -k_5 \end{bmatrix}, \quad \mathcal{Y} = \begin{bmatrix} E \\ I \\ A \\ P \\ H \end{bmatrix},$$

$$\bar{\mathcal{N}}(\mathcal{X}, \mathcal{Y}) = \begin{bmatrix} \kappa \\ 0 \\ 0 \\ 0 \\ 0 \end{bmatrix},$$

and $\kappa = \dfrac{(\alpha_1 I + \alpha_2 A + \alpha_3 P + \alpha_4 H)}{N}(S_0 - S)$.

It is evident that $\mathcal{B}$ is an M-matrix. Since at DFE point each of $S, E, I, A, P, H, R \leq S_0$, thus column matrix $\bar{\mathcal{N}}(\mathcal{X}, \mathcal{Y}) \geq 0$. So, DFE point $\mathcal{P}_0$ is GAS. □

7.3 Global stability at EE

We present the next theorem that shows the global stability of the model (2) at EE point $\mathcal{P}_1$.

Theorem 11 *The EE point $\mathcal{P}_1$ of the model (2) is stable provided $\mathcal{R}_0 > 1$ and unstable when $\mathcal{R}_0 < 1$.*

Proof: We consider a Volterra type Lyapunov function defined as

$$\begin{aligned} \mathrm{L}(S, E, I, A, P, H, R) = &\Big[S - S^1 - S^1 \log \frac{S}{S^1}\Big] + \Big[E - E^1 - E^1 \log \frac{E}{E^1}\Big] \\ &+ \Big[I - I^1 - I^1 \log \frac{I}{I^1}\Big] + \Big[A - A^1 - A^1 \log \frac{A}{A^1}\Big] \\ &+ \Big[P - P^1 - P^1 \log \frac{P}{P^1}\Big] + \Big[H - H^1 - H^1 \log \frac{H}{H^1}\Big] \\ &+ \Big[R - R^1 - R^1 \log \frac{R}{R^1}\Big], \end{aligned}$$

where $\mathcal{P}_1 = (S^1, E^1, I^1, A^1, P^1, H^1, R^1)$ is an endemic equilibrium point.
Taking derivative with respect to time t and simplifying, we get

$$\begin{aligned}\frac{d\text{Ł}}{dt} =&\Big[\frac{S-S^1}{S}\Big]\frac{dS}{dt} + \Big[\frac{E-E^1}{E}\Big]\frac{dE}{dt} + \Big[\frac{I-I^1}{I}\Big]\frac{dI}{dt} + \Big[\frac{A-A^1}{A}\Big]\frac{dA}{dt} + \Big[\frac{P-P^1}{P}\Big]\frac{dP}{dt}\\ &+ \Big[\frac{H-H^1}{H}\Big]\frac{dH}{dt} + \Big[\frac{R-R^1}{R}\Big]\frac{dR}{dt}.\end{aligned}$$

Replacing the time derivatives of state variables with the right hand sides of the ODEs of the model (2), we reach at

$$\frac{d\text{Ł}}{dt} = \xi_1 - \xi_2,$$

where

$$\begin{aligned}\xi_1 =&\Big[\Pi + (c_1+\mu)\frac{(S^1)^2}{S} + c_1 S + (\alpha_5+\alpha_6+\alpha_7+\mu)\frac{(E^1)^2}{E} + \alpha_5 E\\ &+ (\alpha_8+\alpha_9+\mu+\delta_I)\frac{(I^1)^2}{I} + \alpha_6 E + (\varphi_1+\mu)\frac{(A^1)^2}{A} + \alpha_7 E\\ &+ (\varphi_4+\delta_H+\mu)\frac{(H^1)^2}{H} + (\varphi_2+\varphi_3+\delta_P+\mu)\frac{(P^1)^2}{P}\\ &+ \alpha_8 I + \alpha_9 I + \varphi_1 A + \varphi_2 P + \varphi_3 P + \varphi_4 H + \mu\frac{(R^1)^2}{R}\Big],\end{aligned}$$

and

$$\begin{aligned}\xi_2 =&\Big[(c_1+\mu)\frac{(S-S^1)^2}{S} + \Pi\frac{S^1}{S} + (c_1+\mu)S^1 + \frac{(E-E^1)^2}{E}(\alpha_5+\alpha_6+\alpha_7+\mu)\\ &+ \frac{E^1}{E}c_1 S + (\alpha_5+\alpha_6+\alpha_7+\mu)E^1 + \frac{(I-I^1)^2}{I}(\alpha_8+\alpha_9+\delta_I+\mu)\\ &+ \frac{I^1}{I}\alpha_5 E + (\alpha_8+\alpha_9+\mu+\delta_I)I^1 + (\varphi_1+\mu)\frac{(A-A^1)^2}{A} + \frac{A^1}{A}\alpha_6 E\\ &+ (\varphi_1+\mu)A^1 + (\varphi_1+\mu)A^1 + \frac{(P-P^1)^2}{P}(\varphi_2+\varphi_3+\delta_P+\mu) + \frac{P^1}{P}\alpha_7 E\\ &+ (\varphi_2+\varphi_3+\delta_P+\mu)P^1 + \frac{(H-H^1)^2}{H}(\varphi_4+\delta_H+\mu) + \frac{H^1}{H}(\alpha_8 I + \varphi_2 P)\\ &+ (\varphi_4+\delta_H+\mu)H^1 + \mu\frac{(R-R^1)^2}{R} + \mu R^1 + \frac{R^1}{R}(\alpha_9 I + \varphi_1 A + \varphi_3 P + \varphi_4 H)\Big],\end{aligned}$$

Since each of the parameters in model (2) is non-negative, hence we have $\frac{d\text{Ł}}{dt} < 0$ when $\xi_1 < \xi_2$ and $\frac{dL}{dt} = 0$ when $\xi_1 = \xi_2$. The case $\xi_1 = \xi_2$ implies that $S = S^1$, $E = E^1$, $A = A^1$, $P = P^1$, $I = I^1$, $H = H^1$, and $R = R^1$.
So, according to LaSalle's invariance principle, the EE point $\mathcal{P}_1$ is globally asymptotically stable. □

8 Sensitivity analysis

Sensitivity analysis plays a vital role to make the best strategies to control a pandemic. Researchers used the tool of sensitivity analysis to mark the parameters with high sensitivity. There are many techniques defined and used for sensitivity analysis. We use the technique named as normalized sensitivity index or elasticity index [33] defined by

$$S_\gamma = \frac{\gamma}{\mathcal{R}_0}\frac{\partial \mathcal{R}_0}{\partial \gamma}$$

Using this approach, sensitivity analysis of the parameters of the model (2) is given in the Table 2. From table data, we observe that α_3 has the highest sensitivity impact on the reproduction number $\mathcal{R}_0$. α_1, α_7 and φ_3 are other parameters which also have higher influence on the number $\mathcal{R}_0$ as compared to the rest of the parameters.

Transmission Rates	Sensitivity Index	Transmission Rates	Sensitivity Index
Π	0	α_8	-0.0938
μ	-0.4080	α_9	-0.1291
α_1	0.2746	φ_1	-0.0213
α_2	0.0130	φ_2	-0.0996
α_3	0.6732	φ_3	-0.3297
α_4	0.0392	φ_4	-0.0147
α_5	-0.0577	δ_I	-0.0064
α_6	-0.1827	δ_P	-0.0133
α_7	0.3612	δ_H	-0.0114

Table 2: Sensitivity index for $\mathcal{R}_0$.

9 Optimal control strategy-I

The most suitable mathematical theory to resolve the problems related to deploying the best choice to get a certain target is optimal control theory. The theory by Pontryagin and Boltyansikii [34] for optimal control problems has been implemented on various integer and fractional order epidemic models to obtain utmost benefits in taking upcoming decision [35]-[40].

In this section, we design an optimal control problem with a strategy to isolate the infected people from the rest of the population. For isolating or self quarantining the infected individuals, a quarantine compartment $Q(t)$ is added in the existing SEIAPHR model (2). We suppose that the infectious people are isolated at the rates c_1, c_2 and c_3 from symptomatic, asymptomatic and super-spreader compartments respectively. In addition to this, we also assume that the isolated people with sever disease symptoms are hospitalized at the rate c_4. Isolated people also die at the rate μ. With these considerations for the newly introduced compartment $Q(t)$, the model (2) is updated to get the following system of equations.

$$\frac{dS}{dt} = \Pi - \frac{(\alpha_1 I + \alpha_2 A + \alpha_3 P + \alpha_4 H)S}{N} - \mu S, \tag{22a}$$

$$\frac{dE}{dt} = \frac{(\alpha_1 I + \alpha_2 A + \alpha_3 P + \alpha_4 H)S}{N} - (\alpha_5 + \alpha_6 + \alpha_7 + \mu)E, \tag{22b}$$

$$\frac{dI}{dt} = \alpha_5 E - (\alpha_8 + \alpha_9 + c_1 + \mu + \delta_I)I, \tag{22c}$$

$$\frac{dA}{dt} = \alpha_6 E - (\varphi_1 + c_2 + \mu)A, \tag{22d}$$

$$\frac{dP}{dt} = \alpha_7 E - (\varphi_2 + \varphi_3 + c_3 + \mu + \delta_P)P, \tag{22e}$$

$$\frac{dQ}{dt} = c_1 I + c_2 A + c_3 P - (c_4 + c_5 + \delta_Q + \mu)Q, \tag{22f}$$

$$\frac{dH}{dt} = \alpha_8 I + \varphi_2 P + c_4 Q - (\varphi_4 + \delta_H + \mu)H, \tag{22g}$$

$$\frac{dR}{dt} = \alpha_9 I + \varphi_1 A + \varphi_3 P + \varphi_4 H + c_5 Q - \mu R, \tag{22h}$$

with initial conditions

$$\begin{aligned} &S(0) = S_0,\ E(0) = E_0,\ I(0) = I_0,\ A(0) = A_0,\\ &P(0) = P_0,\ Q(0) = Q_0,\ H(0) = H_0,\ R(0) = R_0, \end{aligned} \tag{22i}$$

where initial values $S_0,\ E_0,\ I_0,\ A_0,\ P_0,\ Q_0,\ H_0,\ R_0$ are non-negative.

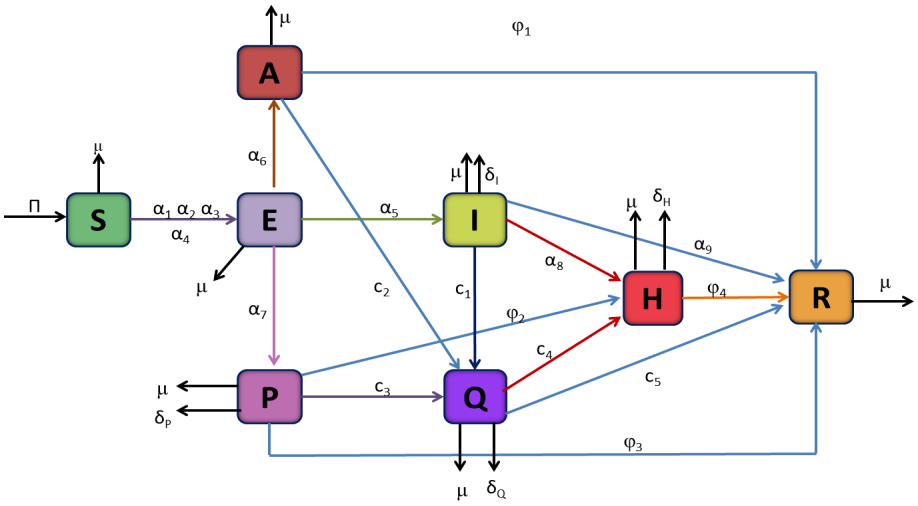

Figure 2: Flow diagram of Covid-19 disease transmission with quarantine class.

The model (22) will serve as restrictions for our optimal control problem. The flow diagram for the model (22) is shown in the Figure 2.

9.1 Cost functional

For formulation of optimal control problem, we consider the cost functional of the following type.

$$\begin{aligned} J(\bar{y}, c) = \int_0^{t_f} \Big[& b_1 I + b_2 A + b_3 P + b_4 Q + b_5 H \\ & + \frac{1}{2}\omega_1 c_1^2(t) + \frac{1}{2}\omega_2 c_2^2(t) + \frac{1}{2}\omega_3 c_3^2(t) + \frac{1}{2}\omega_4 c_4^2(t) \Big] dt, \end{aligned} \tag{23}$$

Here, t_f is final time, $c_i,\ i = 1, 2, 3, 4$ are time-dependent control and $\omega_i,\ i = 1, 2, 3, 4$ are the corresponding costs of controls. The objective of the functional is to reduce the infected individuals with some adjustable costs. The values of constants $b_j,\ j = 1, 2, 3, 4, 5$, will be set either zero or one to have different cost functionals for the sake of analysis.

Our aim is to find optimal control $c^* = (c_1^*,\ c_2^*,\ c_3^*,\ c_4^*) \in \bar{C}$ in the way that cost functional (23) is reduced to its minimum, i.e.,

$$\text{Find } c^* \in \bar{C} \text{ that minimizes } J(\bar{y}, c) \text{ subject to state system (22).} \tag{24}$$

Here $\bar{C}$ is the set of controls specified as

$$\bar{C} = \{c = (c_1, c_2, c_3, c_4) :\ 0 \le c_1, c_2, c_3, c_4 \le 1,\ 0 \le t \le t_f\}.$$

9.2 Necessary conditions

In this section, we formulate a Hamiltonian function in order to derive the necessary optimality conditions for optimal control problem (24). The Hamiltonian $\mathcal{H}$ is described as

$$\mathcal{H}(t, \bar{y}, c, \zeta) = \eta(\bar{y}, c) + \sum_{j=1}^{8} \zeta_j g_j(t, \bar{y}, c),$$

where

$$\eta(\bar{y}, c) = b_1 I + b_2 A + b_3 P + b_4 Q + b_5 H + \frac{1}{2}\omega_1 c_1^2(t) + \frac{1}{2}\omega_2 c_2^2(t) + \frac{1}{2}\omega_3 c_3^2(t) + \frac{1}{2}\omega_4 c_4^2(t),$$

and $\bar{y} = (S, E, I, A, P, Q, H, R)$ symbolize the state variables, $\zeta_j,\ j = 1, 2, 3 \ldots, 8$ are the associated adjoint variables and $g_j(t, \bar{y}, c),\ j = 1, 2, \ldots, 8$ are the right hand sides of the equations of the system (22). Hamiltonian for the control problem (24) in expanded form is written as:

$$\begin{aligned}
\mathcal{H}(t, \bar{y}, c, \zeta) =& b_1 I + b_2 A + b_3 P + b_4 Q + b_5 H + \frac{1}{2}\omega_1 c_1^2(t) + \frac{1}{2}\omega_2 c_2^2(t) + \frac{1}{2}\omega_3 c_3^2(t) + \frac{1}{2}\omega_4 c_4^2(t) \\
&+ \zeta_1 \left(\Pi - \frac{(\alpha_1 I + \alpha_2 A + \alpha_3 P + \alpha_4 H)S}{N} - \mu S \right) \\
&+ \zeta_2 \left(\frac{(\alpha_1 I + \alpha_2 A + \alpha_3 P + \alpha_4 H)S}{N} - (\alpha_5 + \alpha_6 + \alpha_7 + \mu)E \right) \\
&+ \zeta_3 \left(\alpha_5 E - (\alpha_8 + \alpha_9 + c_1 + \mu + \delta_I) I \right) \\
&+ \zeta_4 \left(\alpha_6 E - (\varphi_1 + c_2 + \mu) A \right) \\
&+ \zeta_5 \left(\alpha_7 E - (\varphi_2 + \varphi_3 + c_3 + \mu + \delta_P) P \right) \\
&+ \zeta_6 \left(c_1 I + c_2 A + c_3 P - (c_4 + c_5 + \delta_Q + \mu) Q \right) \\
&+ \zeta_7 \left(\alpha_8 I + \varphi_2 P + c_4 Q - (\varphi_4 + \delta_H + \mu) H \right) \\
&+ \zeta_8 \left(\alpha_9 I + \varphi_1 A + \varphi_3 P + c_5 Q + \varphi_4 H - \mu R \right).
\end{aligned} \tag{25}$$

The first optimality condition

$$\frac{\partial \mathcal{H}}{\partial c} = 0,$$

of the Pontryagin maximum principle provides us the equations for control variables

$$\begin{aligned}
c_1 &= \frac{I(\zeta_3 - \zeta_6)}{\omega_1}, \\
c_2 &= \frac{A(\zeta_4 - \zeta_6)}{\omega_2}, \\
c_3 &= \frac{P(\zeta_5 - \zeta_6)}{\omega_3}, \\
c_4 &= \frac{Q(\zeta_6 - \zeta_7)}{\omega_4}.
\end{aligned}$$

With bounds on controls, we have

$$c_1^* = min\left\{1, max\left\{0, \frac{I(\zeta_3 - \zeta_6)}{\omega_1}\right\}\right\}, \tag{26a}$$

$$c_2^* = min\left\{1, max\left\{0, \frac{A(\zeta_4 - \zeta_6)}{\omega_2}\right\}\right\}, \tag{26b}$$

$$c_3^* = min\left\{1, max\left\{0, \frac{P(\zeta_5 - \zeta_6)}{\omega_3}\right\}\right\}, \tag{26c}$$

$$c_4^* = min\left\{1, max\left\{0, \frac{Q(\zeta_6 - \zeta_7)}{\omega_4}\right\}\right\}. \tag{26d}$$

The second optimality condition

$$\frac{\partial \mathcal{H}}{\partial \bar{y}_j} = -\frac{d\zeta_j}{dt}, \quad j = 1, 2, \ldots, 8,$$

of the Pontryagin maximum principle offers the system of coupled linear adjoint equations:

$$\begin{aligned}\frac{d\zeta_1}{dt} =& \left(\frac{\alpha_1 I + \alpha_2 A + \alpha_3 P + \alpha_4 H}{N} + \mu\right)\zeta_1 \\ & - \left(\frac{\alpha_1 I + \alpha_2 A + \alpha_3 P + \alpha_4 H}{N}\right)\zeta_2,\end{aligned} \tag{27a}$$

$$\frac{d\zeta_2}{dt} = (\alpha_5 + \alpha_6 + \alpha_7 + \mu)\zeta_2 - \alpha_5\zeta_3 - \alpha_6\zeta_4 - \alpha_7\zeta_5, \tag{27b}$$

$$\begin{aligned}\frac{d\zeta_3}{dt} =& \left(\frac{\alpha_1 S}{N}\right)\zeta_1 - \left(\frac{\alpha_1 S}{N}\right)\zeta_2 + (\alpha_8 + \alpha_9 + c_1 + \mu + \delta_I)\,\zeta_3 \\ & - c_1\zeta_6 - \alpha_8\zeta_7 - \alpha_9\zeta_8 - b_1,\end{aligned} \tag{27c}$$

$$\frac{d\zeta_4}{dt} = \left(\frac{\alpha_2 S}{N}\right)\zeta_1 - \left(\frac{\alpha_2 S}{N}\right)\zeta_2 + (\varphi_1 + c_2 + \mu)\,\zeta_4 - c_2\zeta_6 - \varphi_1\zeta_8 - b_2, \tag{27d}$$

$$\begin{aligned}\frac{d\zeta_5}{dt} =& \left(\frac{\alpha_3 S}{N}\right)\zeta_1 - \left(\frac{\alpha_3 S}{N}\right)\zeta_2 + (\varphi_2 + \varphi_3 + c_3 + \mu + \delta_P)\,\zeta_5 \\ & - c_3\zeta_6 - \varphi_2\zeta_7 - \varphi_3\zeta_8 - b_3,\end{aligned} \tag{27e}$$

$$\frac{d\zeta_6}{dt} = (c_4 + c_5 + \delta_Q + \mu)\,\zeta - c_4\zeta_7 - c_5\zeta_8 - b_4, \tag{27f}$$

$$\frac{d\zeta_7}{dt} = \left(\frac{\alpha_4 S}{N}\right)\zeta_1 - \left(\frac{\alpha_4 S}{N}\right)\zeta_2 + (\varphi_4 + \delta_H + \mu)\zeta_7 - \varphi_4\zeta_8 - b_5, \tag{27g}$$

$$\frac{d\zeta_8}{dt} = \mu\zeta_8, \tag{27h}$$

supported with the conditions at final time, i.e.,

$$\zeta_j(t_f) = 0, \quad j = 1, 2, \ldots, 8. \tag{27i}$$

Finally, variation of $\mathcal{H}$ with respect to adjoint variables $\zeta_j,\ j = 1, 2, \ldots, 8$ yield us the ODEs for the state variables as given by (22).

9.3 Solution algorithm

To solve the optimality conditions for the control problem (24), we follow the steps of the following algorithm.

Algorithm 1

1. *Make an initial estimate for the control* $c_j \in C$ *for* $j = 0$.

2. *Approximate solutions of the model* (22) *and the associated adjoint system* (27) *with the control* c_j.

3. *Calculate* $\bar{c}$ *by means of control equations* (26).

4. *Determine new control* $c_j = (\bar{c} + c_j)/2$.

5. *If* $\|\theta_j - \theta_{j-1}\| < \delta\|\theta_j\|$ *for* $j > 0$, *then STOP, otherwise* $j \to j+1$ *and go to step 2.*

θ symbolize the state variables $\bar{y_j}$, adjoint variables ζ_j and the controls c whereas $\delta > 0$ is the tolerance set as per requirement.

9.4 Optimal solutions

This section consists of the presentation and discussion on optimal solutions of the optimal control problem (24). The solutions are obtained by implementing the Algorithm 1 along with Matlab code. State and adjoint variables are approximated usiing RK4. To implement RK4 method,

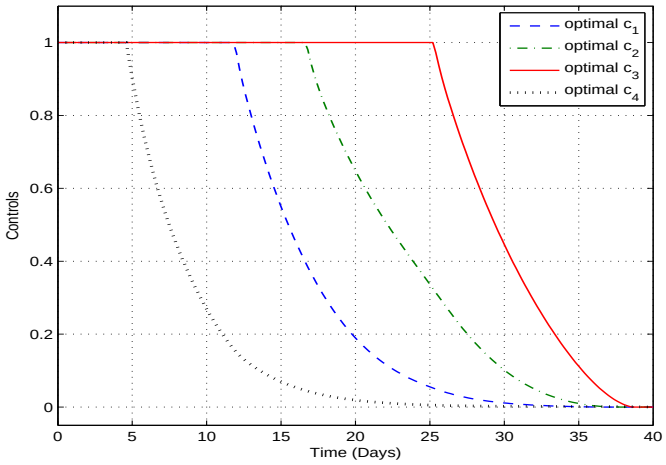

Figure 3: Optimal controls (Case 1).

we discretize continuous time domain $[0, t_f]$ into N equal subintervals each of width $h = \dfrac{t_f}{N} > 0$ such that the corresponding discrete points are given as $t_i = ih,\ i = 0, 1, \ldots, N$. Solutions are approximated at these discrete points. The integral in the cost functional (23) is evaluated by Simpson's $\frac{1}{3}$ formula. For sake of analysis, we consider following two cases of the optimal control problem with two different cost functionals.

Case 1: As a first case, we consider the cost functional (23) with $b_j = 1,\ j = 1, 2, 3, 4, 5$. For this case, the optimizer of the optimal control problem (24) are shown in the Figure 3. These variables respectively offer us the optimum quarantined and hospitalized rates to attain the minimimum cost. Graph for the cost functional is given in the Figure 4. From figure, it is evident that the functional has reached to its minimum under the optimal controls in 14th iteration.

Figure 5 demonstrates graphical curves of state variables before and after optimization. We notice a remarkable decrease in the curves representing exposed, symptomatic, asymptomatic, super-spreader and hospitalized compartments after optimization. The curves from these compartments have moved to disease free state. From the figure, we also observe that there is a need to quarantine and hospitalize more people in the beginning. However, there is in increase in the

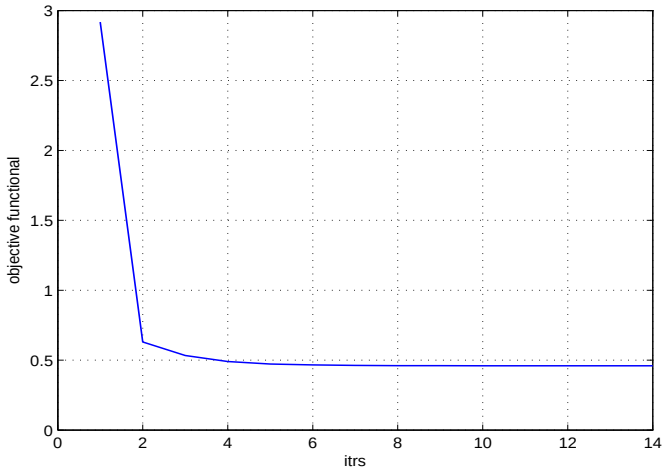

Figure 4: Cost functional (Case 1).

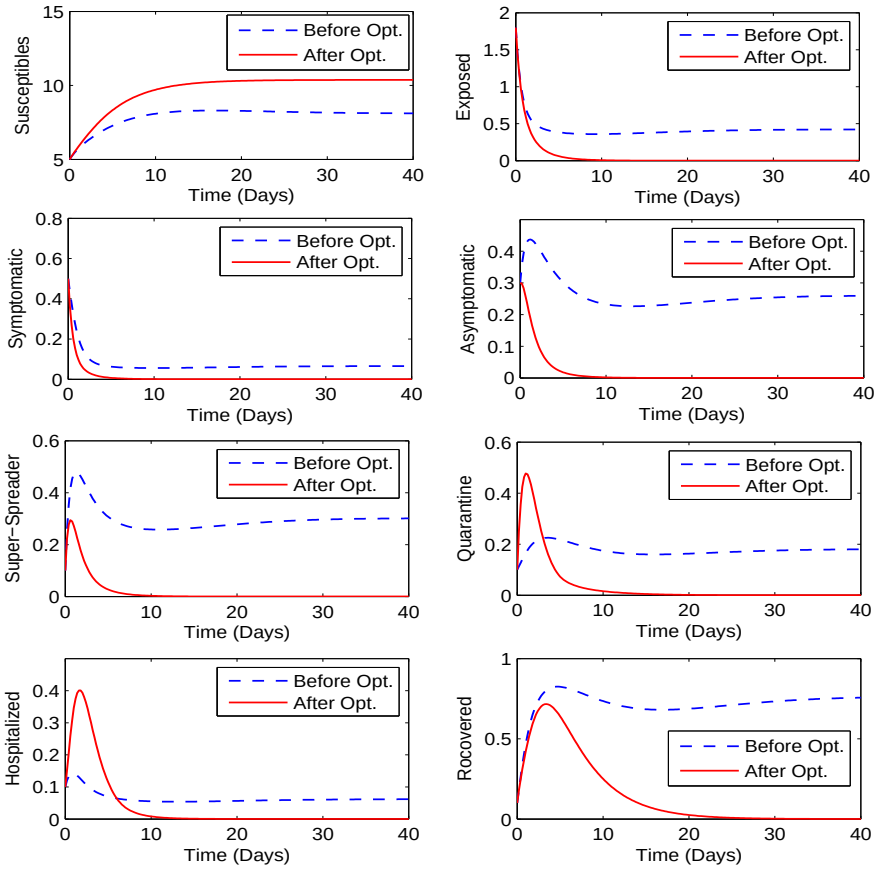

Figure 5: State variables before and after optimization (Case 1).

number of susceptible individuals. Thus, decline in infected individuals is an accomplishment of

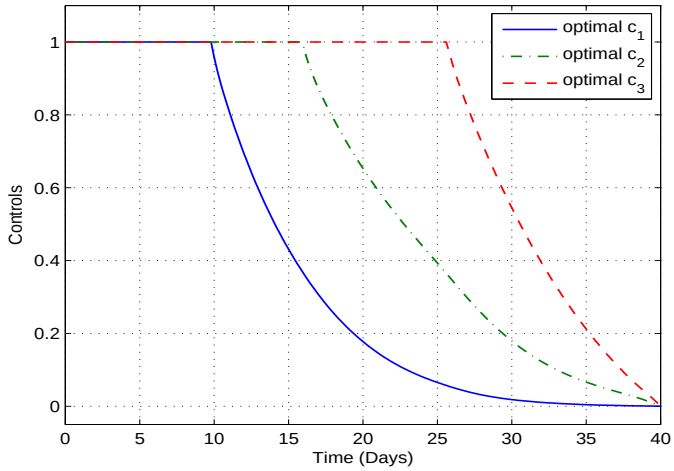

Figure 6: Optimal controls (Case 2).

this optimal control strategy.

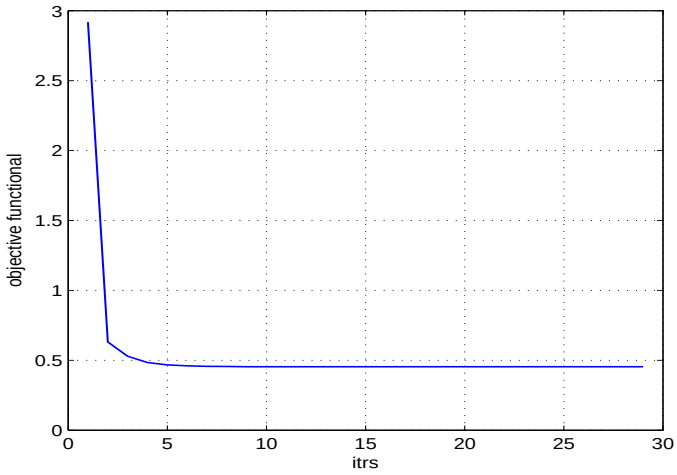

Figure 7: Cost functional (Case 2).

Case 2: Now we consider the cost functional (23) with $b_j = 0$ for $j = 4, 5$ and $b_j = 1$ for $j = 1, 2, 3$. This means that we are not considering the quarantine state Q and the hospitalized class H in cost functional. We also omit the control c_4 from the cost functional. Figure 6 shows the optimal curves for optimizers (control variables c_1, c_2, c_3) of the control problem (24) under assumptions of case 2. We notice that all the controls vary with time but are restricted with in the bounds. The corresponding cost functional (23) with $b_j = 0, \quad j = 4, 5$, shown in Figure 7, approaches to its least value in the 29th iteration of the optimization algorithm.

Figure 8 demonstrates the solution curves of state variables before and after optimization. The solution curves representing exposed, symptomatic, asymptomatic, super-spreader and hospitalized states move to the Corona free state. In addition to this, we also experience a significant drop

of the hospitalized individuals with this case. However, we need to quarantine more individuals in the beginning in order to get optimal reduction in infected individuals.

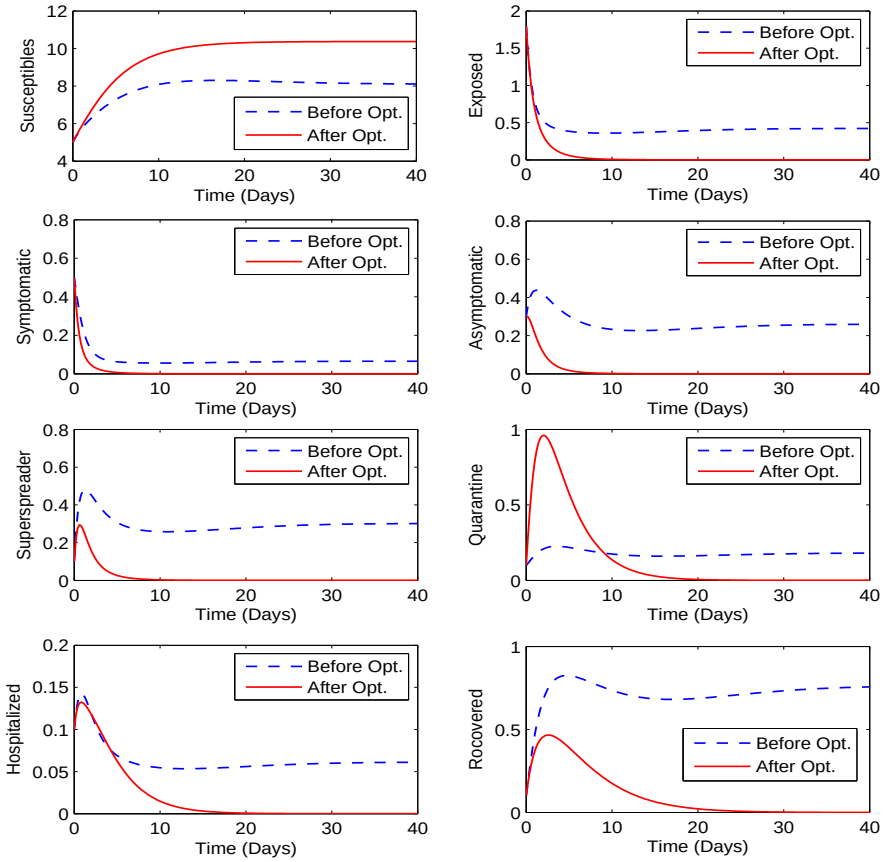

Figure 8: State variables before and after optimization (Case 2).

10 Optimal control strategy-II

The second strategy to control Covid-19 is to tell people about Covid-19 effects, self protection and medication of hospitalized individuals. By educating susceptible about health risks, effects and safety planes of Covid-19, we can restrict the spread of Covid-19. The habit of wearing mask and the practice of social distancing are the key factors of self protection. The best available medicine for the cure of patients with severe condition is also offered to save their lives. To execute this approach, we transform our nonlinear epidemic model (2) to incorporate non-pharmaceutical parameters.

10.1 Modified model

Covid-19 model (2) is restructured to include non-pharmaceutical parameters such as s_1, s_2 and s_3. We assume that susceptible people are recovered at the rate s_1 due to health awareness campaign and the susceptible, exposed, symptomatic, asymptomatic, super-spreader and hospitalized get

well again at the rate s_2 by self protection. The hospitalized individuals move in recovered class at the rate s_3 with possible medication in hospital. With these assumptions, the model (2) is modified to give us the following system of ODEs.

$$\frac{dS}{dt} = \Pi - \frac{(\alpha_1 I + \alpha_2 A + \alpha_3 P + \alpha_4 H)S}{N} - (\mu + s_1 + s_2)S, \tag{28a}$$

$$\frac{dE}{dt} = \frac{(\alpha_1 I + \alpha_2 A + \alpha_3 P + \alpha_4 H)S}{N} - (\alpha_5 + \alpha_6 + \alpha_7 + \mu + s_2)E, \tag{28b}$$

$$\frac{dI}{dt} = \alpha_5 E - (\alpha_8 + \alpha_9 + \mu + \delta_I + s_2)I, \tag{28c}$$

$$\frac{dA}{dt} = \alpha_6 E - (\varphi_1 + \mu + s_2)A, \tag{28d}$$

$$\frac{dP}{dt} = \alpha_7 E - (\varphi_2 + \varphi_3 + \mu + \delta_P + s_2)P, \tag{28e}$$

$$\frac{dH}{dt} = \alpha_8 I + \varphi_2 P - (\varphi_4 + \delta_H + \mu + s_2 + s_3)H, \tag{28f}$$

$$\frac{dR}{dt} = (s_1 + s_2)S + s_2 E + (\alpha_9 + s_2)I + (\varphi_1 + s_2)A + (\varphi_3 + s_2)P + (\varphi_4 + s_2 + s_3)H - \mu R, \tag{28g}$$

with the set of initial conditions:

$$\begin{aligned} &S(0) = S_0,\ E(0) = E_0,\ I(0) = I_0,\ A(0) = A_0, \\ &P(0) = P_0,\ H(0) = H_0,\ R(0) = R_0. \end{aligned} \tag{28h}$$

The model (28) will play the role of a set of restrictions for optimal control problem (30) defined in subsection 10.2. The flow diagram for the model (28) is shown in the Figure 9. To achieve the

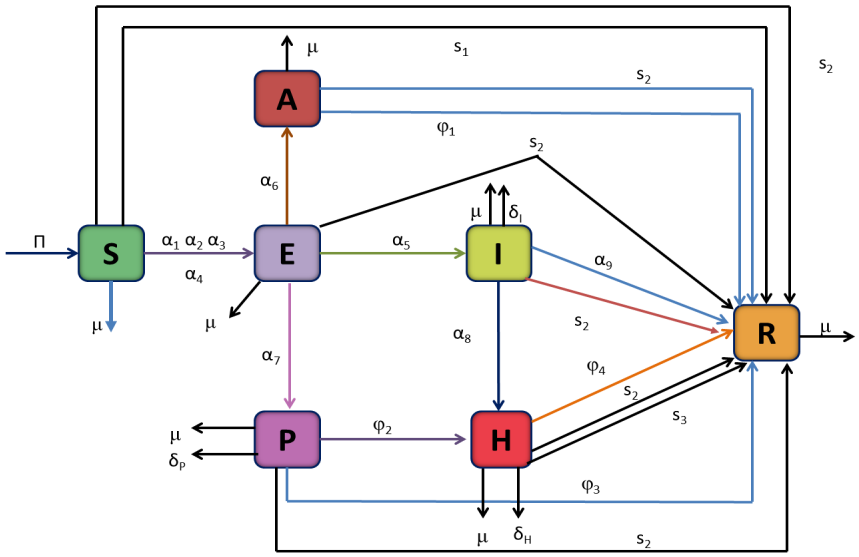

Figure 9: Flow diagram of Covid-19 disease transmission with non-pharmaceutical control parameters.

target of controlling disease with non-pharmaceutical parameters, an optimal control problem is designed by devising a cost functional in the ongoing section. In addition, for the optimal solution of the problem necessary conditions are also computed.

10.2 Cost functional

With the new strategy, the cost functional is defined as follows:

$$J(\tilde{y}, s) = \int_0^{t_f} \Big[a_1 I + a_2 A + a_3 P + a_4 H + \frac{1}{2} W_1 s_1^2(t) + \frac{1}{2} W_2 s_2^2(t) + \frac{1}{2} W_3 s_3^2(t)\Big] dt, \tag{29}$$

where t_f is final time, $s_i,\ i = 1, 2, 3$ represent time-dependent controls, $\tilde{y}$ represent state variables and costs associated with controls are $W_1,\ W_2,\ W_3$.

As our goal is to find optimal control $s^* = (s_1^*,\ s_2^*,\ s_3^*) \in \mathcal{S}$ such that functional (29) is minimized, i.e.,

$$\text{Find } s^* \in \mathcal{S} \text{ that minimizes } J(\tilde{y}, s) \text{ subject to system (28).} \tag{30}$$

$\mathcal{S}$ is the space of controls specified as

$$\mathcal{S} = \{s(t) = (s_1, s_2, s_3) : 0 \le s_1, s_2, s_3 \le 1, 0 \le t \le t_f\}.$$

10.3 Necessary conditions

To build up the necessary conditions for optimal control problem (30), we implement Pontryagin's maximum principle. The optimality conditions are derived from Hamiltonian $\mathcal{H}$ defined as

$$\mathcal{H}(t, \tilde{y}, s, \psi) = \upsilon(\tilde{y}, s) + \sum_{j=1}^{7} \theta_j g_j(t, \tilde{y}, s),$$

where $\upsilon = a_1 I + a_2 A + a_3 P + a_4 H + \frac{1}{2} W_1 s_1^2(t) + \frac{1}{2} W_2 s_2^2(t) + \frac{1}{2} W_3 s_3^2(t)$,
$\tilde{y} = (S, E, I, A, P, H, R)$ symbolize the state variables, related adjoint variables are $\theta_j,\ j = 1, 2, \ldots, 7$ and $g_j(t, \tilde{y}, s),\ j = 1, 2, \ldots, 7$ are the RHS of system (28). Thus, the Hamiltonian for the optimal control (30) is given below.

$$\begin{aligned}
\mathcal{H}(t, \tilde{y}, s, \theta) =& a_1 I + a_2 A + a_3 P + a_4 H + \frac{1}{2} W_1 s_1^2(t) + \frac{1}{2} W_2 s_2^2(t) + \frac{1}{2} W_3 s_3^2(t) \\
&+ \theta_1 \left(\Pi - \frac{(\alpha_1 I + \alpha_2 A + \alpha_3 P + \alpha_4 H) S}{N} - (\mu + s_1 + s_2) S\right) \\
&+ \theta_2 \left(\frac{(\alpha_1 I + \alpha_2 A + \alpha_3 P + \alpha_4 H) S}{N} - (\alpha_5 + \alpha_6 + \alpha_7 + \mu + s_2) E\right) \\
&+ \theta_3 \left(\alpha_5 E - (\alpha_8 + \alpha_9 + \mu + \delta_I + s_2) I\right) + \theta_4 \left(\alpha_6 E - (\varphi_1 + s_2 + \mu) A\right) \\
&+ \theta_5 \left(\alpha_7 E - (\varphi_2 + \varphi_3 + s_2 + \mu + \delta_P) P\right) \\
&+ \theta_6 \left(\alpha_8 I + \varphi_2 P - (\varphi_4 + \delta_H + s_2 + s_3 + \mu) H\right) \\
&+ \theta_7 \left((s_1 + s_2) S + (\alpha_9 + s_2) I + (\varphi_1 + s_2) A + (\varphi_3 + s_2) P\right) \\
&+ \theta_7 \left((\varphi_4 + s_2 + s_3) H - \mu R\right).
\end{aligned} \tag{31}$$

Optimality first condition

$$\frac{\partial \mathcal{H}}{\partial s} = 0,$$

of the Pontryagin maximum principle provides us the equations for control variables

$$
\begin{aligned}
s_1 &= \frac{S(\theta_1 - \theta_7)}{W_1}, \\
s_2 &= \frac{\theta_1 S + \theta_2 E + \theta_3 I + \theta_4 A + \theta_5 P + \theta_6 H - \theta_7 (S + E + I + A + P + H)}{W_2}, \\
s_3 &= \frac{H(\theta_6 - \theta_7)}{W_3},
\end{aligned}
$$

and with bound restriction, updated controls are expressed as

$$s_1^* = min\left\{1, max\left\{0, \frac{S(\theta_1 - \theta_7)}{W_1}\right\}\right\}, \tag{32a}$$

$$s_2^* = min\left\{1, max\left\{0, \frac{\theta_1 S + \theta_2 E + \theta_3 I + \theta_4 A + \theta_5 P + \theta_6 H - \theta_7 (S + E + I + A + P + H)}{W_2}\right\}\right\}, \tag{32b}$$

$$s_3^* = min\left\{1, max\left\{0, \frac{H(\theta_6 - \theta_7)}{W_3}\right\}\right\}. \tag{32c}$$

The second optimality condition

$$\frac{\partial \mathcal{H}}{\partial \tilde{y}_j} = -\frac{d\theta_j}{dt}, \quad j = 1, 2, \ldots, 7,$$

of the Pontryagin maximum principle offers us the system of linear adjoint equations

$$
\begin{aligned}
\frac{d\theta_1}{dt} =& \left(\frac{(\alpha_1 I + \alpha_2 A + \alpha_3 P + \alpha_4 H)}{N} + (\mu + s_1 + s_2)\right)\theta_1 \\
& - \left(\frac{(\alpha_1 I + \alpha_2 A + \alpha_3 P + \alpha_4 H)}{N}\right)\theta_2 - (s_1 + s_2)\,\theta_7, && \text{(33a)} \\
\frac{d\theta_2}{dt} =& (\alpha_5 + \alpha_6 + \alpha_7 + \mu + s_2)\,\theta_2 - \alpha_5\theta_3 - \alpha_6\theta_4 - \alpha_7\theta_5 - s_2\theta_7, && \text{(33b)} \\
\frac{d\theta_3}{dt} =& \left(\frac{\alpha_1 S}{N}\right)\theta_1 - \left(\frac{\alpha_1 S}{N}\right)\theta_2 + (\alpha_8 + \alpha_9 + s_1 + \mu + \delta_I)\,\theta_3 \\
& - \alpha_8\theta_6 - (\alpha_9 + s_2)\theta_7 - a_1, && \text{(33c)} \\
\frac{d\theta_4}{dt} =& \left(\frac{\alpha_2 S}{N}\right)\theta_1 - \left(\frac{\alpha_2 S}{N}\right)\theta_2 + (\varphi_1 + s_2 + \mu)\theta_4 - (\varphi_1 + s_2)\theta_7 - a_2, && \text{(33d)} \\
\frac{d\theta_5}{dt} =& \left(\frac{\alpha_3 S}{N}\right)\theta_1 - \left(\frac{\alpha_3 S}{N}\right)\theta_2 + (\varphi_2 + \varphi_3 + s_2 + \mu + \delta_P)\,\theta_5 - (\varphi_2)\,\theta_6 \\
& - (\varphi_3 + s_2)\theta_7 - a_3, && \text{(33e)} \\
\frac{d\theta_6}{dt} =& \left(\frac{\alpha_4 S}{N}\right)\theta_1 - \left(\frac{\alpha_4 S}{N}\right)\theta_2 + (\varphi_4 + \delta_H + \mu + s_2 + s_3)\,\theta_6 \\
& - (\varphi_4 + s_2 + s_3)\theta_7, && \text{(33f)} \\
\frac{d\theta_7}{dt} =& \mu\theta_7, && \text{(33g)}
\end{aligned}
$$

with conditions at final time

$$\theta_j(t_f) = 0, \quad j = 1, 2, \ldots, 7. \tag{33h}$$

Derivative of Hamiltonian $\mathcal{H}$ with respect to the adjoint variables $\theta_j,\ j = 1, 2, \ldots, 7$, lead us to system of state equations (28).

10.4 Solution algorithm

Optimizer $s^* = (s_1^*, s_2^*, s_3^*)$ of the optimal control problem (30) is determined by implementing the following algorithm.

Algorithm 2

1. *Initially take* $j = 0$ *and set a control* $s_j \in \mathcal{S}$.
2. *Solve the state system* (28) *and the adjoint system* (33) *using control* s_j.
3. *Determine* $\bar{s}$ *using categorization* (32) *of the optimal control.*
4. *Up-date control* $s_j = (\bar{s} + s_j)/2$.
5. *If* $\delta\|\zeta_j\| - \|\zeta_j - \zeta_{j-1}\| \geq 0$ *for* $j > 0$, *then terminate the optimization process, otherwise* $j \to j + 1$ *and go to step 2.*

ζ symbolizes the state variables $\tilde{y}$, adjoint variables θ_j and the control variable s. The parameter δ is the accepted tolerance set as per requirement.

10.5 Optimal solutions

In this section, we present and discuss optimal solutions of the optimal control problem (30). The solutions are obtained by implementing an Algorithm 2 through Matlab code. Time space $[0, t_f]$ is discretized into N equal subintervals each of length $h = \dfrac{t_f}{N} > 0$ with discrete points $t_n = nh,\ n = 0, 1, \ldots, N$. Solutions of state and adjoint equations are obtained at discrete points $t_n,\ n = 0, 1, \ldots, N$ by exploiting RK4 method. Cost functional is approximated by Simpson's 1/3 rule. We categorize here two optimal control problems by considering two different cost functionals each with different controls. For this, we present and discuss the following two cases.

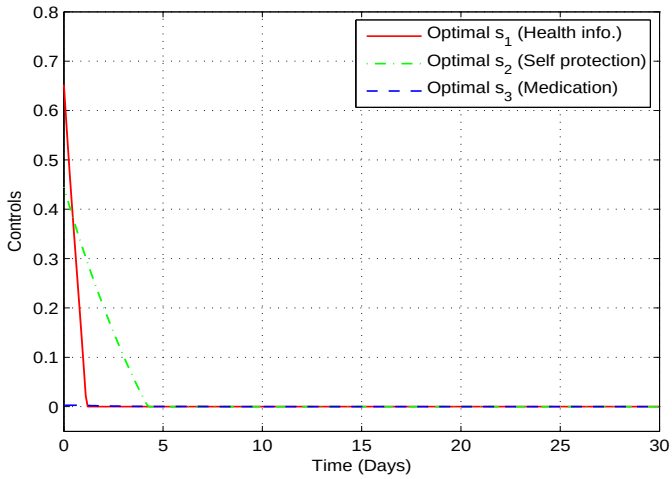

Figure 10: Optimal controls (Case 1).

Case 1: For the first case, we consider all the three controls $s_1,\ s_2$ and s_3 in the cost functional (29). Through Algorithm 2, we get graphs of time dependent optimal control variables as shown in the Figure 10. These are the optimum rates for health information (s_1), self protection (s_2) and medication (s_3) that not only minimize the cost functional but also help in reducing the spread of disease. The graph of cost functional (29) associated with optimization iterations is shown in

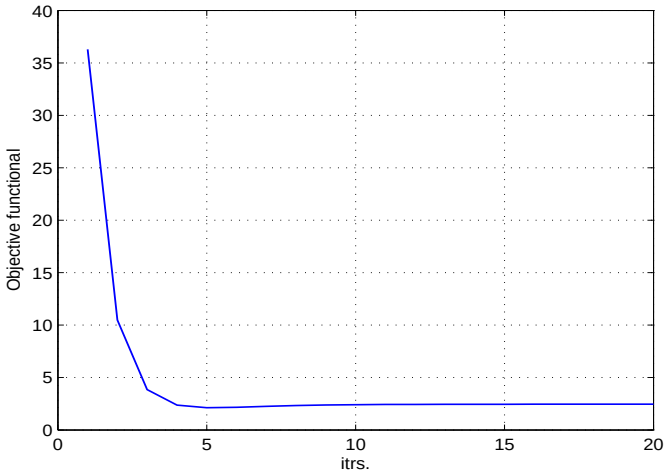

Figure 11: Cost functional (Case 1).

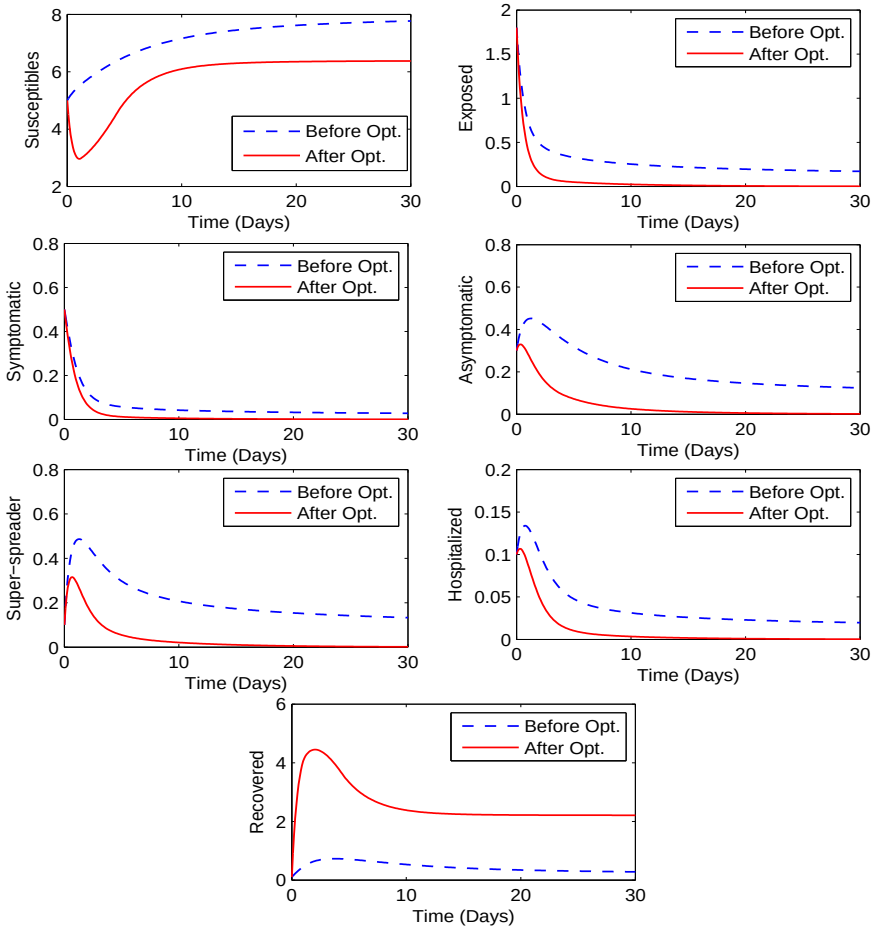

Figure 12: State variables before and after optimization (Case 1).

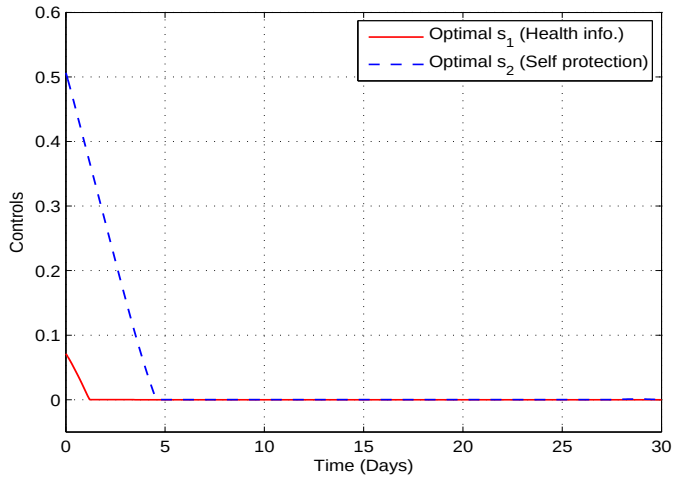

Figure 13: Optimal controls (Case 2).

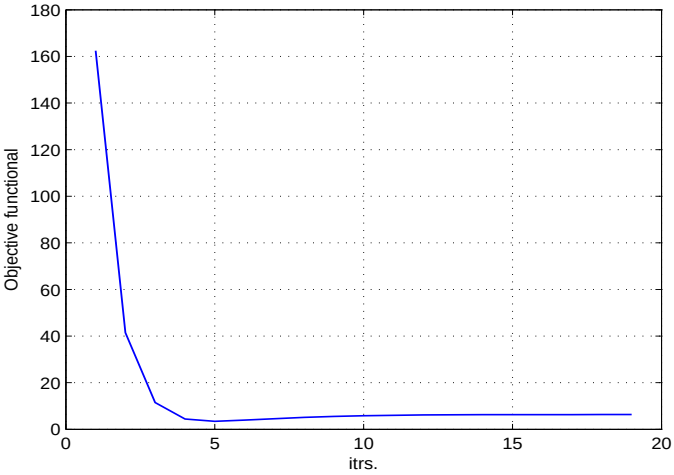

Figure 14: Cost functional (Case 2).

Figure 11. The graph demonstrates that cost functional J has achieved its minimum value with optimal controls shown in Figure 10.

Figure 12 illustrates graphs of state variables before and after optimization. Before optimization, the state variables are computed with some constant controls. From Figure 12, we observe a considerable reduction in the infected individuals in each of the exposed, symptomatic, asymptomatic, super-spreader compartments. In this case, we almost have disease free situation after optimization. However, the figure also shows an increase in the recovered people.

Case 2: In this case, we optimize the optimal control problem (30) by considering only two controls s_1 (health information) and s_2 (self protection). We want to study the effectiveness of the two measures: health information to public and self protection (face masking and social distancing), on the control of disease. In this case, we omit the parameter s_3 from the model

The curves for the optimizers of the control problem (30) are shown in the Figure 13. Under these controls, the cost functional reduced to its minimum value at 19th iteration as shown in the Figure 14.

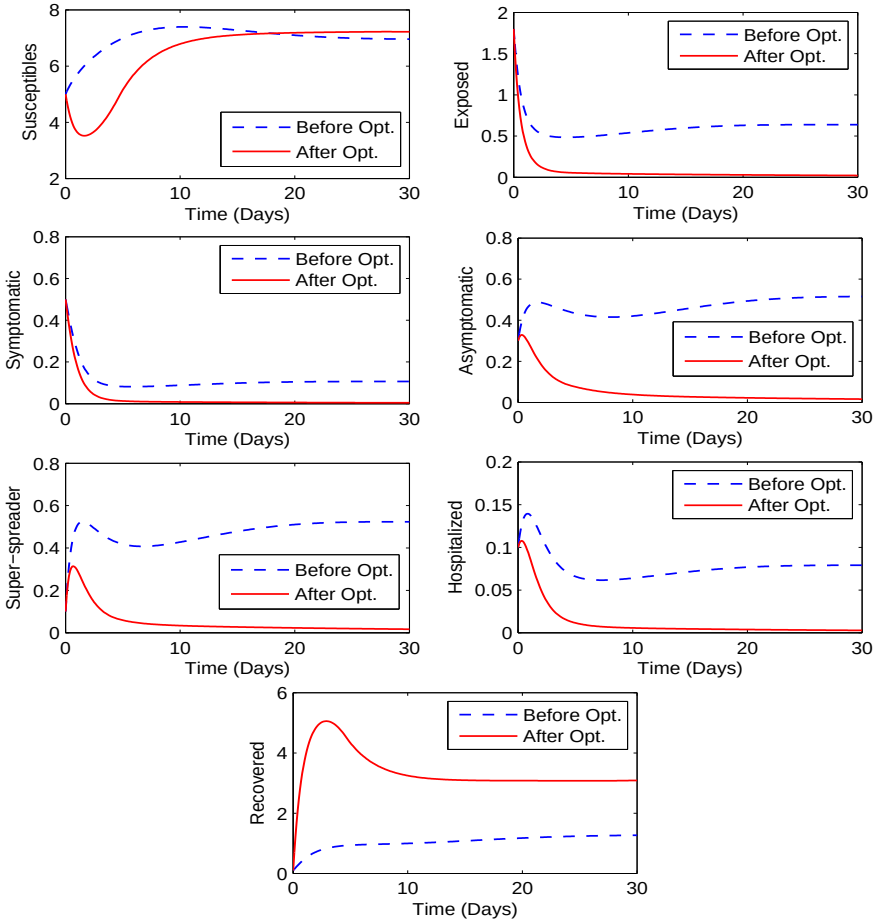

Figure 15: State variables before and after optimization (Case 2).

Behavior of state variables before and after optimization is shown in the Figure 15. State variables before optimization are approximated by using some constant controls. From Figure 15, we observe a reasonable reduction in the infected individuals with the strategy of considering two non-pharmaceutical controls in our model. The rise in susceptible and recovered individuals in this case is more as compared to case 1.

11 Conclusions

In this research work, we designed a nonlinear Covid-19 model not only to study the dynamics of the disease but also to provide a platform for suggesting non-pharmaceutical control strategies for the control of disease. This model is a transformation of the usual SEIR model with a realistic addition of symptomatic, asymptomatic, super-spreader and hospitalization compartments. To study dynamics of the model, we first established that the model has a unique solution and the solutions are non-negative and bounded. We determined reproduction number $\mathcal{R}_0$ as well as the equilibrium points and investigated the local and global stabilities at these points. From sensitivity analysis, we observed that the transmission parameter α_3, rate of transmission of Crona from super-spreader to susceptible, has highest sensitivity index to $\mathcal{R}_0$. To reduce the expansion of the infection, two optimal control strategies were also designed in this study. Primarily, a

quarantine compartment was adjusted in the already designed Covid-19 model with an intention to disconnect the symptomatic, asymptomatic and super-spreaders people from the rest. With this strategy, we considered two cases and studied there the optimum quarantine and hospitalization rates (controls) that restrain the cost functional to minimum. Subsequently, we have experienced a notable decline in the infected curves with this strategy. For the next approach, the typical Covid-19 model was rationalized to acquire three non-pharmaceutical control parameters with an intention to control the disease. By taking into consideration of a new cost functional, we defined an optimal control problem such that the newly added non-pharmaceutical parameters served as control variables. With this strategy, we again discussed two cases by considering different controls. The efficiency of the strategy to control virus is witnessed by simulation results. Conclusively, the second strategy is effortlessly applicable, resourceful and trouble-free to put into practice.

In both of the strategies presented here, we were able to control the spread of disease by reducing the number of infected individuals in exposed, symptomatically infected, asymptomatically infected and super-spreader classes. However, the first strategy looks difficult to implement practically as it requires a reasonable infrastructure and a lot of resources to isolate the huge number of people. Second strategy looks practically possible, as media can play its role in educating people about public health issues as well as about benefits of social distancing and wearing masks.

References

[1] Gralinski LE, Menachery VD. Return of the coronavirus:2019-ncov. Viruses;12:135, 2020.

[2] Barbarossa MV, Fuhrmann J. Meink JH, Krieg S, Varma HV,Castelletti N,et al., Modelling the spread of COVID-19 in Germany: early assessment and possible scenarios. PLoS ONE ;15(9):e0238559, sep 4, 2020.

[3] Nguyen Huy Tuan, Hakimeh Mohammadi, Shahram Rezapour, A mathematical model for COVID-19 transmission by using the Caputo fractional derivative, Chaos, Solitons and Fractals 140:110107, 2020.

[4] WHO. COVID-19 wbpage, 2020b. http://www.covid19.who.it.

[5] C.Buck, A. Llopis, E. Najera, M. Terris, The Challenge of Epidemiology: Issues and slected Readings, vol. 505 of Scientific Publication, Pan American Health Organization, 1998.

[6] Maia Martchva, An Introduction to Mathematical Epidemiology, Springer Science+Bussiness Media New York 2015.

[7] Muhammad Rafique, J.E.Macias-Diaz, Ali Raza, Nauman Ahmed, Design of a nonlinear model for the propagation of COVID-19 and its efficient nonstandard computational implementtation. Applied Mathematical Modeling, 89:1835-1846, 2021:

[8] Faical Ndairo, Ivan Area, Juan J, Nieto, Delfim F.M. Torres., Mathematical modeling of Covid-19 transmission dynamics with a case study of Wuhan. Chaos, Solitons and Fractals, 135: 109846, 2020.

[9] A.I.K. Butt, W. Ahmad, M. Rafiq, D. Baleanu, Numerical analysis of Atangana- Baleanu fractional model to understand the propagation of a novel corona virus pandemic, Alexandria Engineering Journal (2021), doi: https://doi.org/10.1016/j.aej.2021.12.042

[10] A. Hanif, A.I.K. Butt, S. Ahmad, R.U.Din, Mustafa Inc., A new fuzzy fractional order model of transmission of Covid-19 with quarantine class, Eur. Phys. J. Plus, 136:1179, 2021.

[11] Okuonghae D , Omame A . Analysis of a mathematical model for COVID-19 population dynamics in Lagos, Nigeria. Chaos Solitons Fractals, 139:110032, 2020.

[12] Egeonu KU, Omame A, Inyama SC. A co-infection model for two-strain malaria and cholera with optimal control. Int J Dyn Control 2021. doi: 10.1007/ s40435-020-00748-2.

[13] Uwakwe JI, Inyama SC, Omame A. Mathematical model and optimal control of new-castle disease (ND). Appl Comput Math, 9(3):7084,2020. doi: 10.11648/j.acm.20200903.14.

[14] I.A.E. HuiDS , T. Madani , F. Ntoumi , R. Koch , O. Dar , et al. , The continuing 2019-nCoV epidemicthreatof novel coronaviruses to global health: the latest 2019 novel Coronavirus outbreak in Wuhan, China, Int. J. Infect. Dis. 91: 264-266, 2020 .

[15] Ramadan, N., & Shaib, H.. Middle East respiratory syndrome coronavirus (MERS-CoV): A review. Germs, 9(1), 35, 2019.

[16] Yang, C., & Wang, J. A mathematical model for the novel coronavirus epidemic in Wuhan, China. Mathematical biosciences and engineering: MBE, 17(3), 2708 ,2020.

[17] Chowell, G., Fenimore, P. W., Castillo-Garsow, M. A. SARS outbreaks in Ontario, Hong Kong and Singapore: the role of diagnosis and isolation as a control mechanism, & Castillo-Chavez, C. Journal of theoretical biology, 224(1), 1-8, 2003.

[18] Biswas, S. K., Ghosh, J. K., Sarkar, S., & Ghosh, U. COVID-19 pandemic in India: a mathematical model study. Nonlinear dynamics, 102(1), 537-553, 2020.

[19] Hui, D. S., Azhar, E. I., Madani, T. A., Ntoumi, F., Kock, R., Dar, The continuing 2019-nCoV epidemic threat of novel coronaviruses to global health-The latest 2019 novel coronavirus outbreak in Wuhan, China. International journal of infectious diseases, 91, 264-266, 2020.

[20] Araz, S. I, Analysis of a Covid-19 model: optimal control, stability and simulations. Alexandria Engineering Journal, 60(1), 647-658, 2021.

[21] Gupta, H., Kumar, S., Yadav, D., Verma, O. P., Sharma, T. K., Ahn, C. W., & Lee, J. H. Data Analytics and Mathematical Modeling for Simulating the Dynamics of COVID-19 Epidemic-A Case Study of India. Electronics:10, 127, 2021.

[22] Reuters, Wordometer, Coronavirus Incubation Period, available from: https://www.worldmeters. info/coronavirus/coronavirus-incubation-period.

[23] P.-Y. Liu, S. He, L.-B. Rong, S.-Y. Tang, The effect of control measures on COVID-19 transmission in Italy: Comparison with Guangdong province in China, Infectious Diseases of Poverty 9 (2020) 130(1-13).

[24] A. Wilder-Smith, D. O. Freedman, Isolation, quarantine, social distancing and community containment: pivotal role for old-style public health measures in the novel coronavirus (2019-ncov) outbreak, Journal of Travel Medicine 27 (2020) 1-4.

[25] Bajiya VP, Bugalia S, Tripathi JP. Mathematical modeling of COVID-19: Impact of non-pharmaceutical interventions in India. Chaos.30(11):113143, 2020.

[26] Chernet Tuge Deressa, Yesuf Obesie Mussa, Gemechis File Duressa, Optimal control and sensitivity analysis for transmisson dynamics of Coronavirus, Results in Physics 19:103642, 2020.

[27] V.I Arnold. Ordinary Differential Equations. Translated and Edited by Richard A.Silverman. The M.I.T. Press. 1998.

[28] Richard.L.Burden, J. Douglas Faires, Annette M. Burden, Numerical Analysis, CENGAGE Learning, 2014.

[29] Erwin Kreyszig,Introductry Functional Analysis with Application, John wiley and sons, New York, 1993.

[30] Diekmann, J. A. P. Heesterbeek, AND J. A. J. Metz, On the definition and the computation of the basic reproduction ratio R0 in models for infectious diseases in heterogeneous populations, J. Math. Biol., 28:365382, 1990.

[31] W. Ahmad, M. Abbas, Effect of quarantine on transmission dynamics of Ebola virus epidemic: a mathematical analysis, European Physical Journal Plus, Vol. 136, Issue 4, Article no. 355, pp:1-33, 2021.

[32] C. Castillo-Chavez, Z. Feng, W. Huanz, P.V.D. Driessche, D.E. Kirschner, On the computation of RO and its role in global stability, Mathematical Approaches for Emerging and Reemerging Infectious Diseases: An Introduction, IMA, 125, Springer-Verlag, 2002.

[33] Pauline Van Den Drissche, Reproduction numbers of infectious disease models. Infectious Disease Modelling:2,288-303, 2017.

[34] L.S. Pontryagin, V.G. Boltyanskii, The mathematical theory of optimal processes. New York: Golden and Breach Science Publishers; 1986.

[35] Piu Samui, Jayanta Mondal, Subhas Khajanchi., A mathematical modeling of Covid-19 transmission dynamics with a case study of Wuhan. Chaos, Solitons and Fractal:140,110173,2020.

[36] F.B. Agusto, Optimal chemoprophylaxis and treatment control strategies of a tuberculosis transmission model. World J Model Simul. 5:163173, 2009.

[37] K. Fister, S. Lenhart, J. McNally, Optimizing chemotherapy in an HIV model. Electron J Differ Equ. 32:112, 1998.

[38] S. Lenhart, JT Workman, Optimal control applied to Biological models, Chapman & Hall/CRC, 2007.

[39] M.D. Ahmad, M. Usman, A. Khan, M. Imran, Optimal control analysis of Ebola disease with control strategies of quarantine and vaccination, Infectious Disases Poverty, 5:72, 2016.

[40] M.Imran, H. Rafique, A. Khan, T. Malik, A model of bi-mode transmission dynamics of hepatitis C with optimal control, Theory Biosci. 2014. doi:10.1007/s12064-013-0197-0.